The Salinity-Phase-Inversion method (SPI-slope): A straightforward experimental approach to assess the hydrophilic-lipophilic-ratio and the salt-sensitivity of surfactants

Guillaume Lemahieu, Jesus Ontiveros, Théophile Gaudin, Valérie Molinier,
Jean-Marie Aubry

HAL Id: hal-04094015
https://hal.univ-lille.fr/hal-04094015v1

Submitted on 1 Dec 2023

The Salinity-Phase-Inversion method (SPI-slope):
A straightforward experimental approach to assess the hydrophilic-lipophilic-ratio and the salt-sensitivity of surfactants

Guillaume Lemahieu[1], Jesús F. Ontiveros[1*], Théophile Gaudin[1],
Valérie Molinier[2], Jean-Marie Aubry[1*]

(1) *Univ. Lille, CNRS, Centrale Lille, Univ. Artois, UMR 8181– UCCS – Unité de Catalyse et Chimie du Solide, F-59000 Lille, France.*

(2) *Total Exploration Production, Pôle d'Etudes et de Recherche de Lacq, B.P. 47, 64170 Lacq, France.*

jean-marie.aubry@univ-lille.fr, jesus-fermin.ontiveros@centralelille.fr

Abstract

Hypothesis

The salinity at which the dynamic phase inversion of the reference system $C_{10}E_4$ / *n*-Octane / Water occurs in the presence of increasing amounts of a test surfactant S_2 provides quantitative information on the hydrophilic/lipophilic ratio and on the sensitivity to $NaCl_{aq}$ of S_2.

Experiences

The Salinities causing the Phase Inversion (SPI) of the reference system mixed with 12 ionic and 10 nonionic well-defined surfactants are determined in order to quantify the contributions of the nature of the polar head and of the alkyl chain length.

Findings

The SPI varies linearly upon the addition of S_2. The slope of the straight variation with the molar fraction of S_2 is called the "SPI-slope". It quantifies the hydrophilic/lipophilic ratio of S_2 in saline environment and its salt-sensitivity with respect to the reference surfactant $C_{10}E_4$. The SPI-slopes of C_{12} surfactants bearing different polar heads are found to decrease in the following order: $C_{12}NMe_3Br > C_{12}E_8 > C_{12}E_7 > C_{12}SO_3Na \approx C_{12}COONa \geq C_{12}SO_4Na > C_{12}E_6 > C_{12}E_5 > C_{12}PhSO_3Na > C_{12}E_3$. This classification is different from that obtained when the phase inversion is caused by a change in temperature (PIT-slope method) because the addition of NaCl in significant amounts (3 to 10 wt.%) partially screens the ionic heads and diminishes their apparent hydrophilicities. A simple model, valid for all types of nonionic surfactants, is developed on the basis of the HLD_N equation (Normalized Hydrophilic-Lipophilic Deviation) to express the SPI-slope as a function of the hydrophilic/lipophilic ratio ($PACN_2$) and the salinity coefficient (δ_2) of S_2. All studied surfactants are positioned on a 2D map according to the values of their SPI-slope and their PIT-slope to graphically highlight their hydrophilic/lipophilic ratio and their salt-sensitivity. Finally, a linear model connecting the PIT-slope and the SPI-slope is derived for nonionics, emphasizing that the thermal partitioning is much greater in the PIT-slope than in the SPI-slope.

Keywords: Salinity Phase Inversion, SPI-slope, surfactant classification, HLD, salt-sensitivity, optimum formulation.

Abbreviations used in the article:

ACN	Alkane Carbon Number of n-alkanes
Cc	Characteristic curvature of surfactants
C_iE_j	Surfactant $H(CH_2)_i(OCH_2CH_2)_jOH$
CMC	Critical Micelle Concentration of surfactants
$dPIT/dx_2$	PIT-slope of the surfactant under study S_2
$dSPI/dx_2$	SPI-slope of the surfactant under study S_2
DTAB	DodecylTrimethylAmmonium Bromide
EON	Ethylene Oxide Number
EOR	Enhanced Oil Recovery
f_w	Weight fraction of water
HLB	Hydrophilic Lipophilic Balance
HLD	Hydrophilic Lipophilic Deviation
HLD_N	Normalized Hydrophilic Lipophilic Deviation
m_o	Mass of oil (n-octane)
m_{C10E4}	Mass of the reference surfactant ($C_{10}E_4$)
m_w	Mass of water
NAC	Net Average Curvature
O/W	Oil in Water
PACN	Preferred Alkane Carbon Number of surfactants
PIT	Phase Inversion Temperature
S_1	Reference surfactant ($C_{10}E_4$)
S_2	Surfactant under study
S*	Optimal salinity at equilibrium
SOW	Surfactant / Oil / Water system
SPI	Salinity Phase Inversion
W/O	Water in Oil

1. Introduction

Surfactants are ubiquitous in many end-use products (shampoos, cosmetics, food) and applied in several industrial processes (enhanced oil recovery, asphalt emulsion) due to their association properties and their capacity to modify the surface/interfacial tension [1] of liquid/gas, liquid/liquid and liquid/solid systems. Large quantities of these commodities are synthesized every year to satisfy an increasing market and new molecules are developed to offer sustainable alternatives to petro-based traditional surfactants. The choice of the most suitable alternative surfactant for a specific application is complex, because it depends both on its molecular structure but also on its physicochemical environment (composition and ratio of aqueous and oil phases, temperature, salinity, pressure, presence of additives) which modifies significantly its apparent hydrophilic/lipophilic ratio.

Several descriptors have been proposed in order to characterize surfactants in terms of their hydrophilicity/hydrophobicity tendency. The Hydrophilic Lipophilic Balance (HLB) introduced by Griffin in 1949 [2] is an empirical arbitrary scale ranging from 1 (lipophilic) to 20 (hydrophilic) for nonionic surfactants. The HLB can be determined experimentally following a protocol based on the stability of a series of emulsions or calculated using a formula proposed by Griffin for polyethoxylated nonionic surfactants [3]. In 1954 Davies [4] extended the calculation domain of HLB to ionic surfactants

and other nonionic polar groups by using a group contribution method. The HLB is still commonly used in industry due its simplicity although other major formulation variables such as salinity or temperature are ignored in this scale.

Israelachvili *et al.* [5] proposed the packing parameter "p", a theoretical concept based on geometric considerations of the surfactant. This notion, initially designed to predict the shape of the micelles of surfactants in aqueous solution, was subsequently extended to more complex temperature-sensitive Surfactant / Oil / Water (SOW) systems including oil, organic or ionic additives by introducing the so-called "effective packing parameter". However, these concepts, although very effective for interpreting physicochemical behaviour, are of limited use for formulators looking for the most suitable surfactant for a particular application.

The Hydrophilic-Lipophilic-Deviation (HLD), introduced by Salager *et al.* [6], is a semi-empirical model that quantifies the affinity of a given surfactant for the oil and aqueous phases. This equation takes into account most of the formulation variables as the nature of the surfactant and of the oil, the salinity of the aqueous phase, the possible presence of alcohols, and the temperature of the system [7,8]. The parameters of the HLD equation are determined by formulation scans of SOW systems at equilibrium and the complete description of a surfactant requires numerous time-consuming unidimensional scans. The value of HLD can be related to the phase behaviour of SOW systems as well as the type and the stability of the corresponding emulsions [9,10]. When HLD = 0, a SOW system is at its "optimum formulation" and the surfactant has the same affinity for oil and water. Acosta *et al.* [11] re-interpreted the HLD as a descriptor of the interfacial curvature and proposed the Net-Average-Curvature model (HLD-NAC) to reproduce the solubility, the equivalent droplet radius and the interfacial tension of microemulsions. This model uses the same HLD equation, but most publications concerning HLD-NAC rename the original characteristic parameters of the surfactant (σ and β) as the "Characteristic curvature", Cc. These parameters (σ, β and Cc) are useful for practical applications of the HLD equation but their physical meaning is unclear. Therefore, Salager introduced the concept of Preferred Alkane Carbon Number (PACN), [12–15] to express the hydrophilic/lipophilic ratio of the surfactant. This parameter has an understandable physical meaning since it corresponds to the Alkane Carbon Number (ACN) of the n-alcane that provides an optimum formulation under specific standard conditions, namely 25 °C in a SOW system free of alcohol and salt for nonionic surfactants and with 1% of NaCl for ionics.

Surfactant PACNs can be determined accurately provided that the Surfactant / n-Alkane / Water ternary systems lead to so-called "fish diagrams" within the temperature window experimentally accessible [14]. As most surfactants are not able to provide such diagram, it is necessary to resort to an indirect and less accurate method based on the disturbance of a reference SOW system. Thus, Ontiveros *et al.* proposed the "PIT-slope", a simple and fast perturbation method to assess the hydrophilic-lipophilic ratio of surfactants, using the Phase Inversion Temperature (PIT) shifting of the $C_{10}E_4$ / n-Octane / Water reference emulsion. When the surfactant under study S_2 is added to this SOW system, the PIT varies linearly with S_2 concentration and the slope of the line, called "PIT-slope", may be used as a comparative criterion to quantify the hydrophilic/lipophilic ratio of S_2 [16,17]. A positive slope indicates that the test surfactant is more hydrophilic than $C_{10}E_4$ in the reference conditions, whereas a negative value corresponds to the opposite. Many well-defined or technical grade ionic and nonionic surfactants have been characterized by this method that allows comparing new surfactants with various unusual polar heads or alkyl chains [16,17]. The relationship between PIT-slope and HLD equation, established elsewhere [18] show that this method allows estimating the PACN of nonionic surfactants with a precision of ± 2 units.

However, the classification of surfactants based on the sole value of their PIT-slope is insufficient to predict the behaviour of these surfactants under salinity conditions far from that used to perform the measurement ($[NaCl]_{aq}$ = 0.01 M). In particular, the sensitivity to the salinity of surfactants can be of crucial importance for certain applications such as the enhanced oil recovery (EOR). Actually, for EOR, the salinity is the variable of choice to reach the optimum formulation because the temperature is imposed by the reservoir conditions [19]. In this type of application, the salinity of the aqueous phase typically varies between 0.1 and 3 M (0.6 – 17.5 wt.%) and the apparent hydrophilic/lipophilic ratio of ionic surfactants is, therefore, much lower than in the absence of salt due to the screening of the charges of the ionic head by the counterions. EOR is undoubtedly the most emblematic application of salt-effect on surfactants, but it is not the only one. More generally, the sensitivity of surfactants to electrolytes is a key parameter for many other major end-use products such as detergents or personal care products. For example, the current method of imparting significant viscosity to shampoos consists of finely adjusting their salinity in order to increase the packing parameter of the mixture of surfactants and to convert spherical micelles to more viscous wormlike micelles.

For the EOR application, discontinuous salinity scan at the well temperature is the standard method to test different mixtures of surfactants in order to get ultra-low interfacial tension with a specific crude oil. Most of the published data regarding salt scans of SOW systems have been performed by observing the phase behaviour at equilibrium (Winsor I, II or III) of a series of tubes maintained at constant temperature and containing increasing concentrations of NaCl. In practice, the so-called "optimum salinity" (noted S*) is visually detected by locating the balanced three-phase system (WIII) which contains equal volumes of water and oil in the middle microemulsion phase. These particular conditions also correspond to the minimum O/W interfacial tension. These scans require, in some cases, lengthy equilibrium times to unambiguously identify the phase behaviour with complex oils. Also, some SOW systems do not lead to three-phase microemulsion systems but rather form gels or viscous phases over the salinity gradient. In addition, this protocol does not provide any information on the physicochemical modifications occurring close to the optimum formulation. Finally, as the variations in salinity are discontinuous, the optimum salinity can only be approached and not determined accurately.

Salager *et al.* [20] showed that the optimum salinity S* of a SOW system at equilibrium coincides with the change of the morphology (from O/W to W/O) of the emulsions, obtained by stirring the contents of the previous pre-equilibrated system. On the basis of this result, the so-called dynamic SPI (Salinity Phase Inversion) method was developed recently by replacing the discontinuous salinity scan by a continuous scan so as to cause the phase inversion. The term "dynamic" is used here to indicate that the salinity of the stirred SOW mixture is changed continuously and not step by step as in the traditional "static" SPI method where a series of tubes containing increasing concentrations of salt are kept at constant temperature until phase equilibrium. The dynamic SPI method, much faster than the traditional stepwise method, has already proven its effectiveness in optimizing the formulation of technical-grade EOR surfactant blends in the presence of crude oil in the salinity range 50-150 g/L at temperatures from 40 to 65°C [19]. The phase inversion was induced either by increasing continuously the salinity of a stirred SOW system or by diluting the brine with water to decrease the salinity. In both cases, oil and surfactant must be added at the same time to keep the proportions of water, oil and surfactant constant. The salinity at which the morphology of the emulsion switches from O/W to W/O (or vice versa) is called "SPI" (a concept analogous to the PIT). The S* (static method) and SPI (dynamic method) values are almost similar if the Water/Oil volume ratios are close to 1.

In the present work, a dynamic salinity scan is employed to quantify the hydrophilic/lipophilic ratio and the salt sensitivity of well-defined ionic and nonionic surfactants. The principle of the method is based on the disturbance of the SPI induced by a test surfactant S_2 to a known SOW reference system consisting of 3 wt% $C_{10}E_4$ / n-Octane / Brine. This method is conceptually similar to the PIT-slope method previously described [16,17] except that the scanning variable is the salinity of the aqueous phase rather than the temperature. The disturbance is quantified by the slope of the SPI linear variation as a function of the molar fraction x_2 of S_2. A simple model, valid for all types of nonionic surfactants, is developed on the basis of the HLD (Hydrophilic-Lipophilic Deviation) equation to express the SPI-slope as a function of parameters characterizing the hydrophilic/lipophilic ratio of the surfactant under study S_2 and its salt sensitivity. The final purpose is to assess the hydrophilic/lipophilic ratio and the salt-sensitivity of surfactants bearing various ionic and nonionic polar heads bound to alkyl chain of different lengths. Finally, the information provided by the SPI-slope and PIT-slope methods are compared graphically in a 2D map and rationalized on the basis of a physicochemical model considering the effective hydrophilic/lipophilic ratio of the mixture of surfactants located at the O/W interface.

2. Experimental

Chemicals

Pure tetraethyleneglycol monodecyl ether ($C_{10}E_4$) used as the reference surfactant (S_1) was synthesized according to a method described elsewhere [21,22]. Its purity was assessed by NMR and GC analyses (> 99%) and by comparing its cloud point temperature [23] (20.4 °C at 2.6 wt%) with the reference value (20.6 °C at 2.6 wt%). n-Octane (99%) was obtained from Sigma-Aldrich. Sodium chloride NaCl ($\geq$ 99.5%) was supplied by Acros Organics. The surfactants studied in this work (named S_2 thereafter), which are listed in Table 1, were used without further purification. Tridecanoic acid sodium salt was obtained in aqueous solution by neutralization of tridecanoic acid (Sigma-Aldrich $\geq$ 98%) with stoichiometric amount of sodium hydroxide.

Table 1 List of the studied surfactants S_2

Surfactant	Abbreviation	Supplier	Purity
Pentaethylene glycol monoctyl ether	C_8E_5	Sigma	> 98%
Tetraethylene glycol monodecyl ether	$C_{10}E_4$	Our lab	> 99%
Pentaethylene glycol monodecyl ether	$C_{10}E_5$	Sigma	> 97%
Triethylene glycol monododecyl ether	$C_{12}E_3$	TCI	> 95%
Tetraethylene glycol monododecyl ether	$C_{12}E_4$	TCI	> 98%
Pentaethylene glycol monododecyl ether	$C_{12}E_5$	Fluka	> 98%
Hexaethylene glycol monododecyl ether	$C_{12}E_6$	Sigma	> 98%
Heptathylene glycol monododecyl ether	$C_{12}E_7$	TCI	> 95%
Octaethylene glycol monododecyl ether	$C_{12}E_8$	TCI	> 95%
Pentaethylene glycol monotetradecyl ether	$C_{14}E_5$	Fluka	> 99%
Sodium Dodecylsulfate	$C_{12}SO_4Na$	Acros	99%
Sodium 1-Dodecanesulfonate	$C_{12}SO_3Na$	Alfa Aesar	99%
Tridecanoic Acid Sodium Salt	$C_{12}CO_2Na$	Our lab	> 98%
Sodium dodecylbenzenesulfonate	$C_{12}PhSO_3Na$	TCI	> 98%
Sodium Oleate	$C_{17:1}CO_2Na$	Sigma	> 99%
Potassium Oleate	$C_{17:1}CO_2K$	TCI	> 98%
Octyltrimethylammonium Bromide	$C_8 NMe_3Br$	Fluka	98%
Decyltrimethylammonium Bromide	$C_{10} NMe_3Br$	Alfa Aesar	> 98%

Surfactant	Abbreviation	Supplier	Purity
Dodecyltrimethylammonium Bromide	$C_{12} NMe_3Br$	Alfa Aesar	99%
Tetradecyltrimethylammonium Bromide	$C_{14} NMe_3Br$	Alfa Aesar	> 98%
Hexadecyltrimethylammonium Bromide	$C_{16} NMe_3Br$	Acros	> 99%
Octadecyltrimethylammonium Bromide	$C_{18} NMe_3Br$	TCI	98%

Preparation and preconditioning of samples

Before the SPI-slope experiment, 0.26 g (m_{S1}) of the reference surfactant $C_{10}E_4$, 4.25 g (m_w) of water and 4.25 g (m_o) of n-octane were introduced in a 20 mL vial (d = 2.5 cm, h = 5.5 cm). This $C_{10}E_4$ / n-Octane / Water mixture (8.8 g, 10.5 mL) was vigorously shaken by hand during a few seconds and left to pre-equilibrate 1 h at 20.0 °C before performing the salinity phase inversion. Other samples were prepared by adding, to the pre-conditioned SOW system, small amounts (mass m_{S2}) of the surfactant under study S_2 in order to cover the range 0-1.5 wt%. The amount of $C_{10}E_4$ is adjusted to m_{S1} during the measurement so that the proportion of S_1 surfactant remains constant at 3 wt% of the whole mixture.

Salinity Phase Inversion (SPI)

The salinity phase inversion experiments were carried out at 20.0 °C inside a thermostated cell already described [19] and shown in Figure 1. The system was kept under continuous stirring at 800 rpm using a magnetic cross bar stirrer (diameter 1.8 cm). The program performs a real time acquisition at *ca.* 2 data per second. To continuously modify the salinity, a concentrated aqueous solution of NaCl (25 wt%, $\rho_1 = 1.189$ g/mL) was added to the initial SOW mixture at a controlled flow rate Q_i of 0.05 mL/min thanks to a press-syringe engine model 78-8100INT from KdScientific® fitted with a 10-mL Terumo-syringe (reference SS+10ES1). Simultaneously, *n*-octane ($\rho_2 = 0.703$ g/mL) containing 6 wt% of $C_{10}E_4$ was introduced in the same way at 0.083 mL/min flow rate to maintain a constant water weight fraction f_w and a constant surfactant concentration. The conductivity and temperature were simultaneously monitored by a Radiometer Analytical CDM 210 conductometer fitted with a CDC741T platinised platinum probe. The software used was custom written in a Labview 7.1 National Instruments platform. Salinity and conductivity profiles were obtained as a function of time.
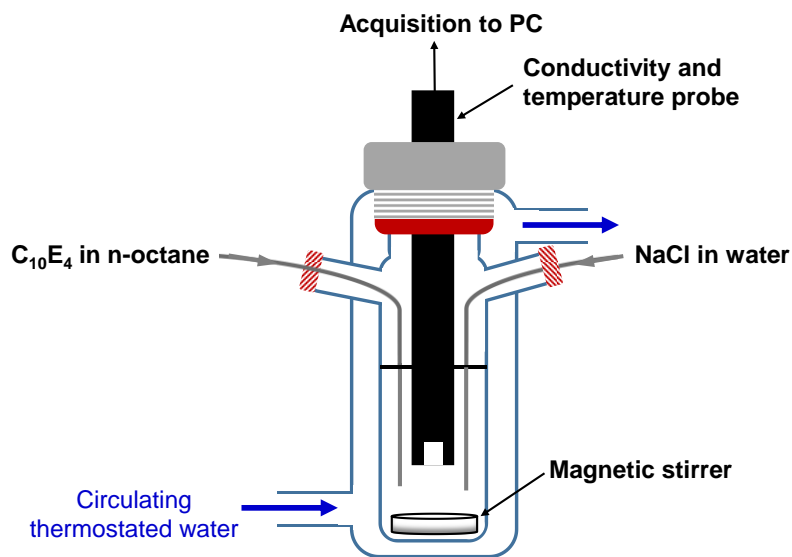

Fig. 1. Thermostated cell used to perform salinity phase inversions at 20.0 °C [19]. An aqueous solution of NaCl (25 wt%) and a solution of $C_{10}E_4$ (6 wt%) in octane are injected into the cell at controlled flow-rates thanks to press-syringes in order to maintain f_w equal to 0.5.

The water weight fraction f_w defined by equation (1) is 0.5 in all systems.

$$f_w = \frac{m_w}{m_w + m_o} \tag{1}$$

The aqueous phase salinity S(t), expressed in grams of NaCl per 100 g of aqueous phase, can be calculated at each time of the experiment by the following relation (2).

$$S(t) = \frac{S_0 m_{w0} + t.S_1 Q_1 \rho_1}{m_{w0} + t.Q_1 \rho_1} \times 100 \tag{2}$$

Where S_0 and S_1 are the initial and the added aqueous phase salinity respectively, t is the time (in min), m_{w0} (in g) the initial aqueous weight, Q_1 (in mL.min^{-1}) the flow-rate of aqueous solution added to the SOW system and ρ_1 is the density of the of the aqueous NaCl solution (1.19 g/mL). In the same way, the amount of the surfactant S_2 changes with time, and the value at the phase inversion can be determined by the relation (3).

$$S_{2,SPI} wt.\% = \frac{m_{S2,0}}{m_0 + t_{SPI}(Q_1.\rho_1 + Q_2.\rho_2)} \times 100 \tag{3}$$

where $S_{2,SPI} wt\%$ is the weight concentration of S_2 at the phase inversion and $m_{S2,0}$ (g) is the amount of the surfactant S_2 at the beginning; m_0 (g) the initial mass of the entire SOW system; ρ_1 and ρ_2 (g/mL) are respectively the density of the aqueous NaCl solution and the n-octane 6 wt% $C_{10}E_4$ solution (0.70 g/mL); Q_2 (mL/min) is the flow-rate of the oil added to the SOW system. The molar fraction of S_2 at the inversion is calculated with equations 4 and 5.

$$x_{2,SPI} = \frac{m_{S2,SPI}/MW_2}{m_{S1,SPI}/MW_1 + m_{S2,SPI}/MW_2} \tag{4}$$

$$m_{S1,SPI} = m_{S1,0} + t_{SPI}(Q_2.\rho_2) \cdot 0.06 \tag{5}$$

The SPI values are determined from the conductivity curves by using the parallel tangent method and are given with a precision of $\pm$ 0.5 g/L. Numeric examples of mass balances calculated with Eq. 1-5 are detailed in Supplementary Material.

3. Results

The phase behaviour of the $C_{10}E_4$ / n-Octane / Water at equilibrium has been described in literature by Kahlweit *et al.* [24,25] and Pizzino *et al.* [26] using temperature as formulation variable. The effect of salinity in C_iE_j / Water systems depends on the nature and concentration of the added electrolytes. As NaCl is a salting-out electrolyte, its addition to C_iE_j / Water and C_iE_j / Oil / Water systems diminishes the cloud point and shifts the fish diagram to lower temperatures [27]. As a consequence, the addition of NaCl to such SOW system maintained at constant temperature induces the WI$\rightarrow$ WIII$\rightarrow$ WII transition. In order to observe this transition, the choice of the temperature for the salinity scan is critical. It must be lower than the fish-tail temperature T* of the reference $C_{10}E_4$ / n-Octane / Water system (25.7 °C [26]) to guarantee that the phase behaviour is effectively a WI without salt at the start of the scan. Therefore, the work temperature was fixed at 20.0 °C since Lemahieu *et al.* [19] showed that, at this temperature, the 3% $C_{10}E_4$ / n-Octane / NaCl$_{(aq)}$ system at f_w=0.5 presents a three-phase behaviour (WIII) in the 1.5-4.9 wt% NaCl range. The phase inversion was located according to two protocols, the standard one in which the conductivity is measured separately for a series of pre-emulsified samples with different salinities and the dynamic one in which the salinity is changed continuously in the same sample under stirring. With both methods, the salinity phase inversion (SPI) takes places at 3.3 ± 0.2

wt% NaCl.

3.1. Influence of the added surfactant S_2 on the SPI of the $C_{10}E_4$ / n-Octane / Water system.

Figure 2 shows the conductivity vs. salinity profiles for two well-defined polyethoxylated dodecyl surfactants ($C_{12}E_j$) added to the 3% $C_{10}E_4$ / n-Octane / Water reference system under stirring. The profiles resemble the one observed by Salager *et al.* during a discontinuous salinity scan of the SDS / n-Pentanol / Kerosene / Brine system [9]. However, the curves obtained with the continuous scan exhibit some irregularities just before and after the phase inversion which were not detected with the discontinuous protocol [28]. In the first part of the curve, the conductivity is high and increases sharply with salinity in accordance with an O/W emulsion morphology. Then, in a narrow salinity range, the conductivity drops dramatically, indicating a phase inversion towards a W/O emulsion. In every conductivity profile of Figure 2, a conductivity bump appears just after the fall, which is usually attributed either to the temporary occurrence of liquid crystals or to a complex morphology resulting from the agitation of the WIII system [29–31]. In Figure 2A the conductivity bump is tiny but, for the last profile of Figure 2B, the two peaks of conductivity are equivalent, a phenomenon already reported by Kahlweit *et al.* [25] when the water fraction is extremely high (f_w = 0.9) and the lamellar phase is crossed during a temperature scan for the 15% $C_{10}E_4$ / n-Octane / 0.01 wt% $NaCl_{aq}$ system. In order to test this explanation, an equilibrated system corresponding to the salinity of the second bump was prepared but no liquid crystal was observed.
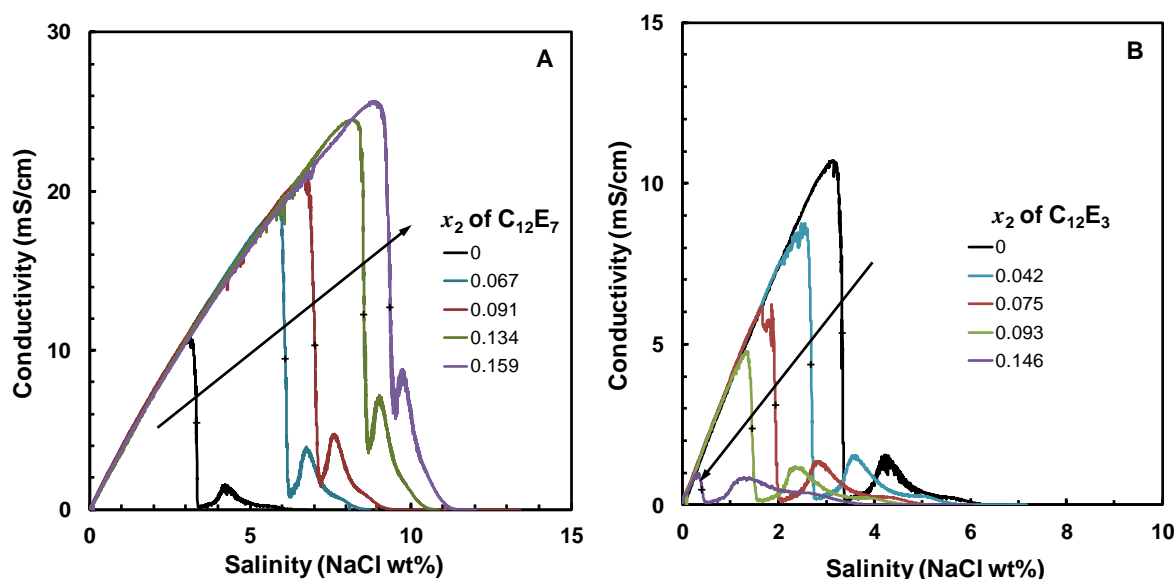

Fig. 2. Salinity-dependence of the conductivity of the (3 wt% $C_{10}E_4$+S_2) / n-Octane / $NaCl_{aq}$ systems with increasing molar fraction of S_2 at fw = 0.5 and T=20.0 °C. A) S_2 = $C_{12}E_7$. B) S_2 = $C_{12}E_3$. The SPI is represented as "+" on the curves at different molar fractions.
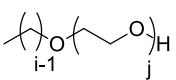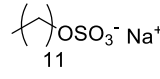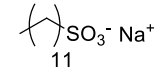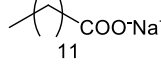
When increasing amounts of $C_{12}E_7$ are added to the reference SOW system, the SPI also increases (Fig. 2A). An opposite behaviour is observed when $C_{12}E_3$ is added (Fig. 2B). The cloud temperature of $C_{12}E_7$ is 65 °C [32] whereas it is lower than 0 °C for $C_{12}E_3$. Compared to the value of 20.4 °C for $C_{10}E_4$, it is clear that $C_{12}E_7$ is more hydrophilic and $C_{12}E_3$ is less hydrophilic than $C_{10}E_4$. At constant temperature, Bourrel *et al.* [13] and Kahlweit *et al.* [33] have demonstrated that the more hydrophilic the nonionic surfactant is, the more salt has to be added to achieve a three-phase behaviour. The increase in the SPI observed for the $C_{10}E_4$/$C_{12}E_7$ mixture and the decrease for the $C_{10}E_4$/$C_{12}E_3$ mixture confirms that the
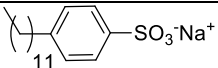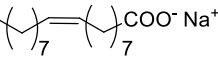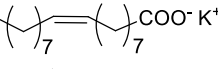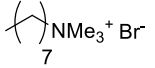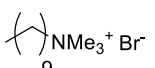
hydrophilic/lipophilic ratio of these three surfactants is in the order $C_{12}E_7 > C_{10}E_4 > C_{12}E_3$ regardless the scanned variable, temperature or salinity. This result, expected for such surfactants, will not necessarily hold true for surfactants with more dissimilar hydrophilic heads. In summary, the hydrophilic/lipophilic ratio of the test surfactant S_2 relative to $C_{10}E_4$ in the salinity range investigated determines whether the SPI increases or decreases as the proportion of S_2 is increased in the amphiphilic mixture $C_{10}E_4 + S_2$.

3.2. The "SPI slope", a new descriptor of ionic and nonionic surfactants

In most cases, the evolution of the SPI with the molar fraction x_2 of the added surfactant S_2 is well fitted by a linear regression. The slope of this line, $dSPI/dx_2$, is called the SPI-slope by analogy to the PIT-slope, previously described [17]. The latter corresponds to the l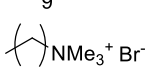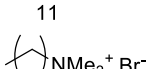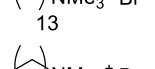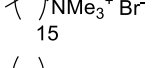inear evolution of the Phase Inversion Temperature (PIT) when increasing amounts of S_2 is added to the reference system $C_{10}E_4$ / n-Octane / Water. The SPI-slope was used to assign a score to some twenty well-defined ionic or nonionic surfactants. The results are summarized in Table 2 along with the already known PIT-slope values to allow a comparison of the two classification scales. The practical interest of these descriptors for rationalizing the behaviour of surfactants in aqueous solution or in SOW systems will be discussed at a qualitative level in the results section and, in more detail, in the discussion part, on the basis of a simple physicochemical model of the O/W interfacial film.

Table 2 SPI-slope ($dSPI/dx_2$) and PIT-slope ($dPIT/dx_2$) [17] of well-defined nonionic and ionic surfactants

Surfactant	Structure	SPI-slope / wt% NaCl	PIT-slope / °C
$C_{12}E_3$		-20.5	-27
$C_{12}E_4$		-7.3	-9.2
$C_{12}E_5$		7.2	6.8
$C_{12}E_6$		22.3	33
$C_{12}E_7$		38.0	63
$C_{12}E_8$		51.9	98
$C_{10}E_4$		0	0
$C_{14}E_5$		2.4	1.6
$C_{10}E_5$		15.0	22
C_8E_5		21.3	34
$C_{12}SO_4Na$		27.8	499
$C_{12}SO_3Na$		35.6	516
$C_{12}CO_2Na$		35.5	409

Surfactant	Structure	SPI-slope / wt% NaCl	PIT-slope / °C
$C_{12}PhSO_3Na$		3.5	409
$C_{17:1}CO_2Na$		14.5	253
$C_{17:1}CO_2K$		19.8	347
C_8NMe_3Br		53.3	54
$C_{10}NMe_3Br$		80.7	338
$C_{12}NMe_3Br$		66.4	486
$C_{14}NMe_3Br$		57.0	453
$C_{16}NMe_3Br$		47.9	426
$C_{18}NMe_3Br$		43.0	-

Influence of the polar head on the SPI-slope of ionic and nonionic surfactants with dodecyl chain.

The influence of the nature of the polar head on the SPI-slope was studied by comparing a series of ionic and nonionic surfactants having identical C_{12} hydrophobic chains linked to various hydrophilic groups. Figure 3 shows the variation of SPI as a function of the molar fraction x_2 of the test surfactant S_2 for six well-defined polyethoxylated dodecanol ($C_{12}E_j$) and four ionic surfactants (anionic or cationic). A linear regression fits well the experimental data for both polyethoxylated ($R^2 > 0.99$) and ionic dodecyl surfactants ($R^2 > 0.98$). At the same molar fraction, the SPI of the nonionic surfactants $C_{12}E_j$ increases with the number of ethoxy groups, as expected. With typical anionic surfactants such as $C_{12}CO_2Na$, $C_{12}SO_4Na$ and $C_{12}SO_3Na$ the difference in the value SPI at the same molar fraction could be interpreted as the result of the difference in the "apparent" hydrophilicity of the polar heads through salinity scan.
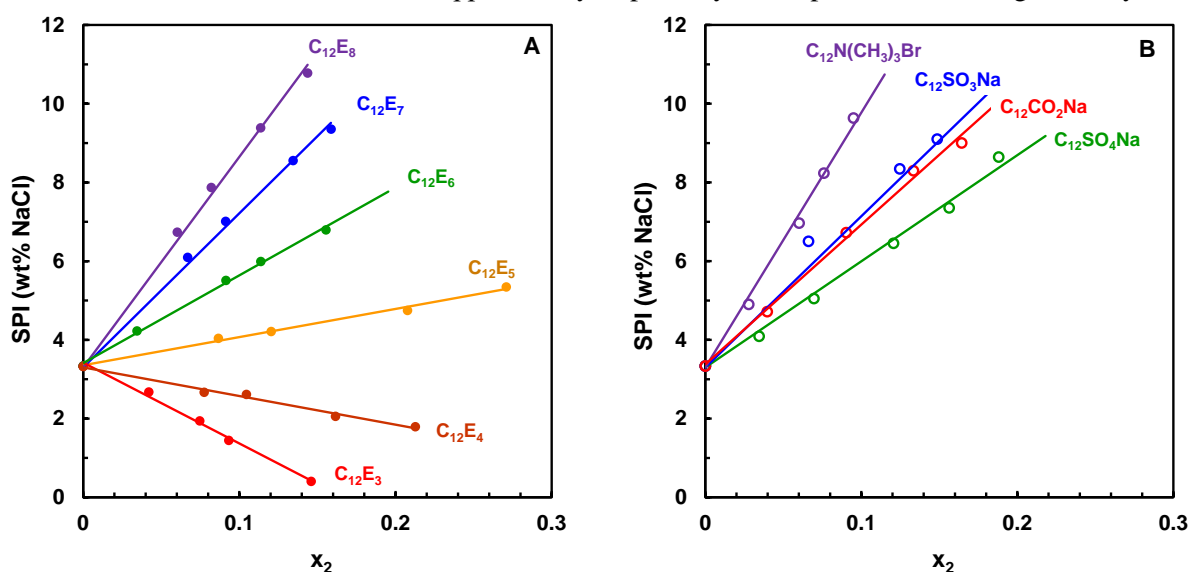
Fig. 3. Evolution of the Salinity Phase Inversion (SPI) as a function of the molar fraction x_2 of various nonionic (A) and ionic (B) surfactants with dodecyl chains. The surfactants under study S_2 are added to the reference system 3% $C_{10}E_4$ / n-Octane / $NaCl_{aq}$ at $f_w = 0.5$ and $T = 20.0$ °C. The slopes of the solid lines, obtained by linear fitting of the experimental points, provide the SPI-slopes values
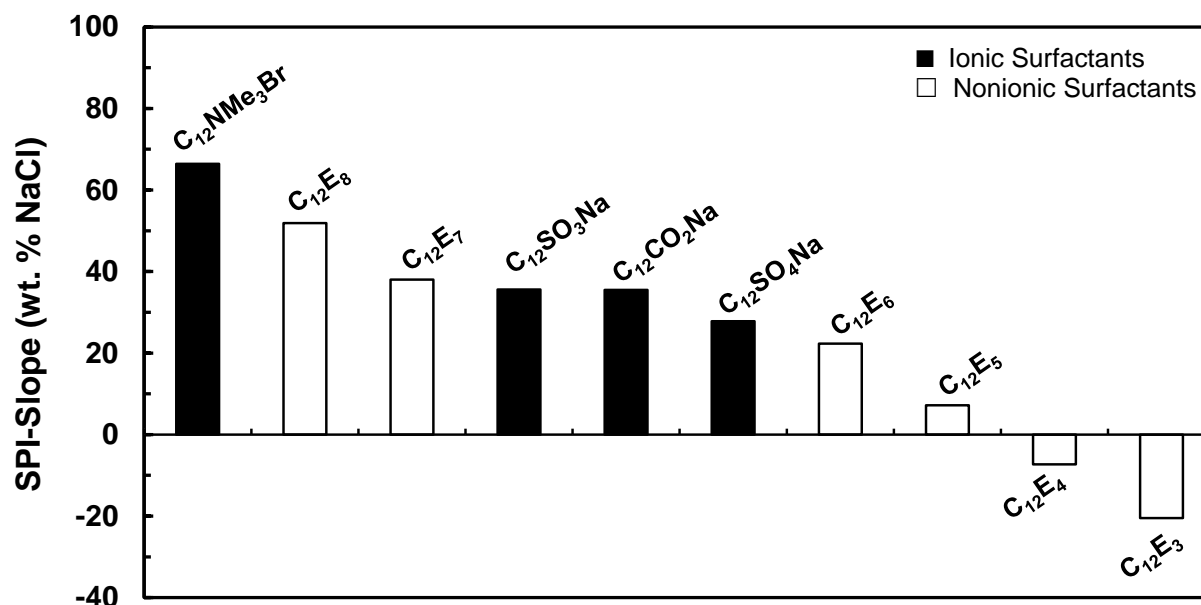

Fig. 4 SPI-slope of well-defined ionic and nonionic surfactants with dodecyl chains and different polar heads

Figure 4 compares in an enlightening way the SPI-slope of the ten surfactants with a *n*-dodecyl chain. On the one hand, if ionic and nonionic surfactants are considered separately, the order is quite consistent with the reported hydrophilicities of the polar heads. In particular for ionic surfactants, this order matches well with the data published from salinity scans at equilibrium for Ionic Surfactant / n-Octane / Butanol / Brine systems [34,35]. Thus, Bourrel and Schechter indicate that the "optimum salinity" decreases in the following order according to the ionic group: $NMe_3Br \gg SO_3Na \geq SO_4Na \geq CO_2Na$. However, the authors specify that *"differences between RSO₃Na, RSO₄Na and RCOONa is not large"* as actually shown in Figure 4. Interestingly, it can be noticed in Figure 4 that the dodecyltrimethylammonium bromide (DTAB) surfactant has a significantly higher SPI slopes compared to other ionic surfactants. This could result from the well-known intrinsic hydrophilicity of the quaternary ammonium group but also, in part, from the bromide counter-anion. Indeed, this relatively large anion with a low charge density has a stronger affinity than the chloride ion for the large quaternary ammonium cation. According to Holmberg, this phenomenon induces a better competitiveness for the interface of the quaternary ammonium bromide compared to the corresponding chloride [36]. In the context of the SPI-slope experiments, it is possible that, in the case of the DTAB surfactant, the bromide counter-ion is hardly substituted by chloride counter-ions, resulting in higher stability of the interfacial environment upon addition of NaCl. By contrast, for other anionic surfactants with sodium counter-ions, such an effect cannot occur.

On the other hand, if the SPI-slopes of ionic surfactants are compared with that of nonionic surfactants, the classification is very different from that obtained from their PIT-slope (see Table 2) and from that usually accepted by physical-chemists and formulators. For instance, it is *a priori* surprising that $C_{12}E_8$ appears substantially more hydrophilic than SDS according to their respective SPI-slope (52 vs. 28 wt% NaCl) while the reverse is true if one considers their PIT-slopes (100 vs. 500 °C). This apparent

contradiction can be explained by the conditions under which the PIT-slope and the SPI-slope are measured. In the first case, the aqueous solution contains just the minimum amount of NaCl (0.01 mol/L = 0.06 wt%) necessary to ensure a sufficient ionic conductivity of the O/W emulsions without modifying the hydrophilicity of the polar heads. On the contrary, the tested SOW system used for the SPI-slope measurements can contains up to 12 wt% (2 mol/L) of NaCl during the experiment. In such concentrated electrolyte solutions, the ionic heads undergo a significant screening of their charge by the counterions, which dramatically diminishes their effective hydrophilicity, while the much more salt-tolerant polyethoxylated chains, retain a large part of their intrinsic hydrophilicity.

That means that the PIT-slope and the SPI-slope provide different and complementary information regarding the phase behaviour of surfactants. The first expresses the intrinsic hydrophilic/lipophilic ratio of the surfactants in low-salinity environments, while the second better distinguishes the surfactants according to their sensitivity to electrolytes. In the discussion section, quantitative relationships between on the one hand, the thermal-sensitivity and salt-sensitivity of surfactants and, on the other hand, the values of the PIT-slope and the SPI-slope will be established.

Influence of the alkyl chain length on the SPI-slope

The influence of the alkyl chain length on the SPI-slope was studied on two homologous series of nonionic and cationic surfactants, the penta(ethylene glycol) n-alkyl ethers (C_iE_5) and the n-alkyltrimethylammonium bromides (C_nNMe_3Br). Figures 5A and 5B show the evolution of the SPI-slope with the number of carbons of the alkyl chains while Figures 5C and 5D shows the evolution of the PIT-slope for comparison. For the nonionic C_iE_5 series (Figures 5A and 5C), both the SPI-slope and the PIT-slope decrease monotonically as the length of the alkyl chain increases. This is the expected evolution since the increase in the hydrophobicity of a surfactant whose polar head is unchanged decreases its hydrophilic/lipophilic ratio.
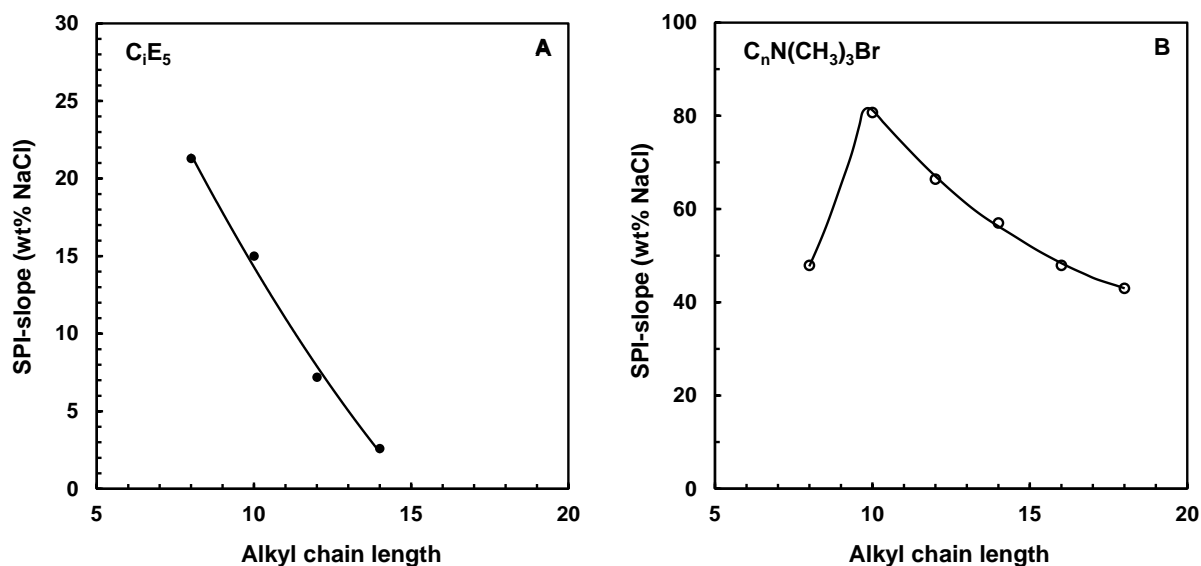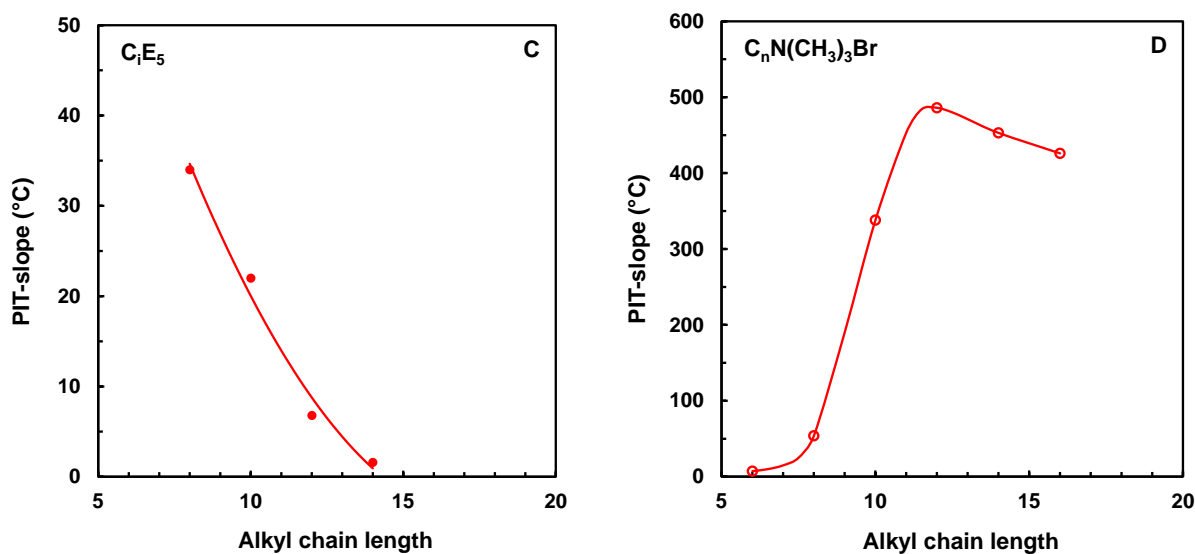
Fig. 5 Evolution of the SPI-slope with increasing alkyl chain length of penta(ethylene glycol) n-alkyl ether C_iE_j (A) and n-alkyltrimethylammonium bromide $C_nN(CH_3)_3Br$ (B) for the system (3% $C_{10}E_4$ + S_2) / n-Octane / Brine at f_w = 0.5 and T = 20.0 °C. The evolutions of the PIT-slope with increasing chain length of the same series of surfactants are shown in C and D for comparison. Continuous curves only serve to guide the eye.

For ionic surfactants (Figures 5B and 5D), the evolution is more complex since the SPI-slope and the PIT-slope first rise sharply when the tail length increases, then it decreases regularly in accordance with the increase of the surfactant hydrophobicity. The octyltrimethylammonium bromide is a very hydrophilic amphiphile which exhibits high monomolecular solubility in water (CMC = 0.14 mol/L = 3.5 wt.%) [37]. Therefore, a significant fraction of the added surfactant partitions into water instead of being located in the interfacial film next to $C_{10}E_4$. As a consequence, the mixed interfacial film ($C_{10}E_4$ + S_2) that drives the phase inversion is less hydrophilic and the measured SPI-slope is lower than expected. For longer chains, the surfactants are mainly localized at the interface and become more and more lipophilic with increasing the chain length. It is worth noting, that the evolutions of the PIT-slopes for both families of surfactants are almost similar to that of the SPI-slope except that the phenomenon of partitioning towards the water phase of the cationic surfactants is even enhanced since it occurs also for the decyl chain.

All these results show that the SPI-slope of a surfactant depends not only on its intrinsic hydrophilic/lipophilic ratio but also on its sensitivity to salt and its partitioning between the interfacial film, the aqueous phase and the n-octane phase.

4. Discussion

The principle of the SPI-slope (and of the PIT-slope) is based on the perturbation of the $C_{10}E_4$ / n-Octane / Water reference system, initially at the optimum formulation, to which increasing percentages of a test surfactant S_2 are added. As a result, S_2 unbalances the system and the salinity (or the temperature) of the system must be readjusted to restore the optimum formulation. Therefore, at phase inversion (SPI or PIT) the system is again at optimum formulation and, if left to equilibrate, it would give a three-phase system of the Winsor III type as depicted in Scheme 1 at different scales.
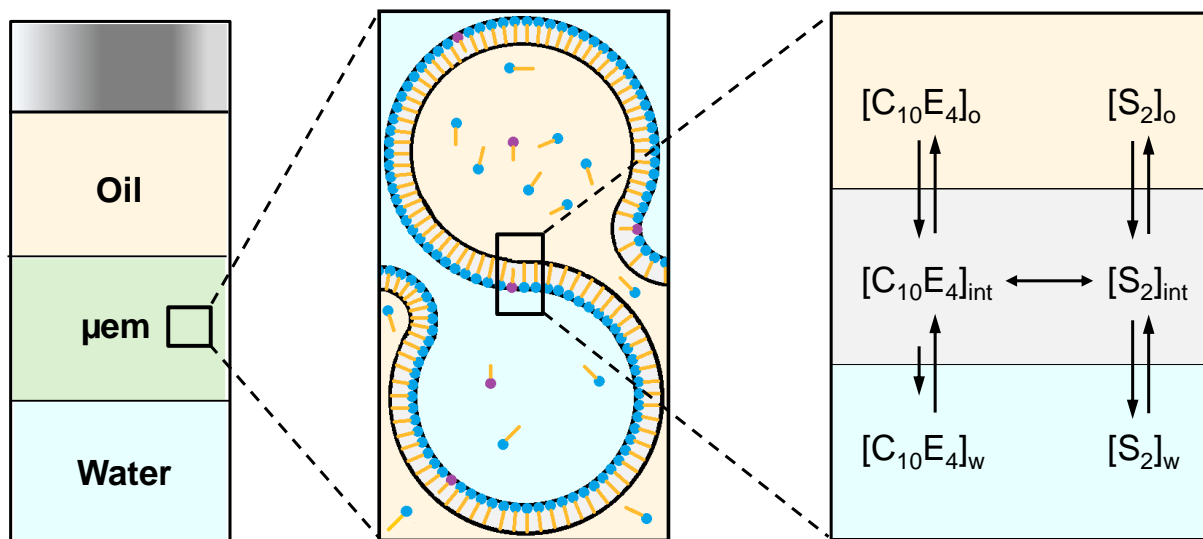
Scheme 1: Macroscopic, nanoscopic and molecular description of a SOW system at the optimum formulation. The surfactants $C_{10}E_4$ (reference) and S_2 constituting the interfacial film (grey) are in equilibrium with the same compounds present in a monomolecular state in the oil (yellow) and water (blue) domains.

On a macroscopic scale, the optimum system spontaneously forms three phases. The middle phase is a bicontinuous microemulsion containing the major part of the surfactants and equal amounts of water and oil. It coexists with an aqueous and an oil excess phases containing monomeric surfactant molecules. At the nanoscopic scale, the microemulsion consists of water and oil nanodomains separated by a highly fluctuating monolayer of surfactants with a zero-mean curvature. At the molecular scale, this monolayer can be regarded as a pseudo-phase of surfactants in equilibrium with monomolecular surfactant molecules dissolved in the oil and water nanodomains. The in-depth analysis of this complex system would require knowing all the equilibria involving surfactants partitioning between the pseudo-phase, the oil and water as well as the evolution of the equilibrium constants as a function of the salinity (or of temperature. Such a study is well outside the scope of this work and the available experimental data are insufficient to calculate all these equilibrium constants.

In the following paragraphs, the experimental findings described above will be rationalized on the basis of the HLD equation. In a first step (section 4.1), a physicochemical model simpler than that depicted in Scheme 1 will be developed for nonionics. More specifically, the equilibria of the surfactants $C_{10}E_4$ and S_2 between the interfacial film and the water and oil excess phases will be neglected as well as the possible interactions between $C_{10}E_4$ and S_2 at the interface (Scheme 1). In a second step (section 4.2), this model will be refined to consider the partitioning of $C_{10}E_4$ between the interfacial film and the excess oil phases. Note that, when S_2 is an ionic surfactant, such a theoretical treatment could not be developed because the HLD of nonionic surfactants varies linearly as a function of salinity and logarithmically for ionic surfactants. Finally, we will highlight how combining SPI-slope and PIT-slope measurements can provide unique insights of the amphiphilic properties of surfactants by positioning a series of well-defined surfactants on a 2D map.

4.1 "Additive" model for nonionic surfactants

In this section, a simple but crude "additive" model is developed assuming that both surfactants $C_{10}E_4$

and S_2 introduced into the medium remain at the O/W interface without partitioning in the aqueous and oil phases and do not undergo significant attractive or repulsive interactions.

Normalized Hydrophilic-Lipophilic-Deviation HLD$_N$ for nonionic surfactants

The effective affinity of a surfactant for the oil and the water phases of a SOW system depends not only on its molecular structure but also on the nature of the oil, the temperature, the salinity of the aqueous phase and the possible presence of amphiphilic additives such as alcohols. Under specific experimental conditions corresponding to the so-called "optimum formulation", the surfactant has an equal affinity for both phases and many special events occur for such SOW systems [14]:

- for equilibrated systems, the average spontaneous curvature of the interfacial film is zero and the interfacial tension γ_{ow} between the oil and water phases exhibits a deep minimum,
- for pre-emulsified systems, the viscosity and stability of the emulsions are minimal and this is also the zone in which the phase inversion occurs.

To help formulators in finding optimum conditions, Salager developed a phenomenological relationship called HLD (Hydrophilic-Lipophilic-Deviation) including the most important formulation variables and expressing quantitatively the deviation of a given SOW system from the optimum formulation [35]. Eq. 6 shows the standard way to write the HLD expression for a system C_iE_j / *n*-Alkane / NaCl$_{aq}$.

$$HLD = (\alpha - EON) - kACN + bS + c_T(T - 25) \qquad (6)$$

Where

- α expresses the hydrophobicity of the surfactant tail.
- EON is the number j of ethoxy units in the hydrophilic head.
- ACN is the Alkane Carbon Number when the oil is an *n*-alkane and k is a numerical coefficient that depends on the sensitivity of the surfactant to variations in ACN.
- S is the salinity of the aqueous phase in wt% of NaCl and b is a numerical coefficient that depends on the surfactant sensitivity to salinity.
- T is the temperature in °C and c_T is a numerical coefficient expressing the sensitivity of the surfactant to temperature

Approximate values of these coefficients have been published in the literature for C_iE_j surfactants ($\alpha \approx 2 + 0.34i$, $k \approx 0.15$, $b \approx 0.13$ wt%$^{-1}$ and $c_T \approx 0.06$ °C^{-1} [35]. In practical terms, the zero value of HLD is a crucial reference point because it corresponds to the conditions for which the SOW system is optimum. As only the optimum formulation (HLD = 0) has a clear physicochemical definition, the expression (6) can be divided by any coefficient and still be equal to zero at the optimum formulation. Thus, dividing equation (6) by the coefficient k results in the "normalized" HLD noted HLD$_N$ (Eq. 7) which is valid for all nonionic surfactants including those whose hydrophilic heads do not contain ethoxy groups.[14,15]

$$HLD_N = PACN - ACN + \delta S + \tau(T - 25) \qquad (7)$$

Where,

- PACN = $(\alpha - EON)/k$ expresses the hydrophilic/lipophilic ratio of the surfactant at 25°C without salt nor co-surfactant
- $\delta = b/k$ reflects the sensitivity of the surfactant towards salinity
- $\tau = c_T/k$ reflects the sensitivity of the surfactant towards temperature

The relationship (7) is simpler and more meaningful than the traditional expression (6) as the deviation from the optimum formulation HLD$_N$ is now expressed in ACN units [14]. Such a scale is unambiguous since, by definition, the ACN of an *n*-alkane oil is equal to its number of carbons regardless the type of

surfactant. Writing the HLD$_N$ in the form (7) has also the advantage of giving an understandable physical meaning to the PACN of a surfactant. Thus, the *"Preferred Alkane Carbon Number" (PACN) of a surfactant corresponds to the number of carbon atoms of the n-alkane (or a mixture of n-alkanes) which gives an optimum formulation at 25 °C in the absence of salt and co-surfactant.*

Determination of the salinity coefficient δ for nonionics

The δ and τ coefficients of a given surfactant can be determined experimentally by carrying out ACN scans with a series of n-alkane oils. Thereby, δ is obtained by studying Surfactant / *n*-Alkane / Water systems maintained at constant temperature whose salinity is adjusted to obtain the optimum salinity (SPI). Likewise, τ is determined from the same SOW systems at constant salinity whose temperature is adjusted to find the optimum temperature (PIT). Such experiments were carried out to determine the δ and τ coefficients of the reference surfactant C$_{10}$E$_4$ through the detection of the optimum formulations by phase inversion (Figure 6) of the SOW system induced by salinity scan (SPI) or temperature scan (PIT).
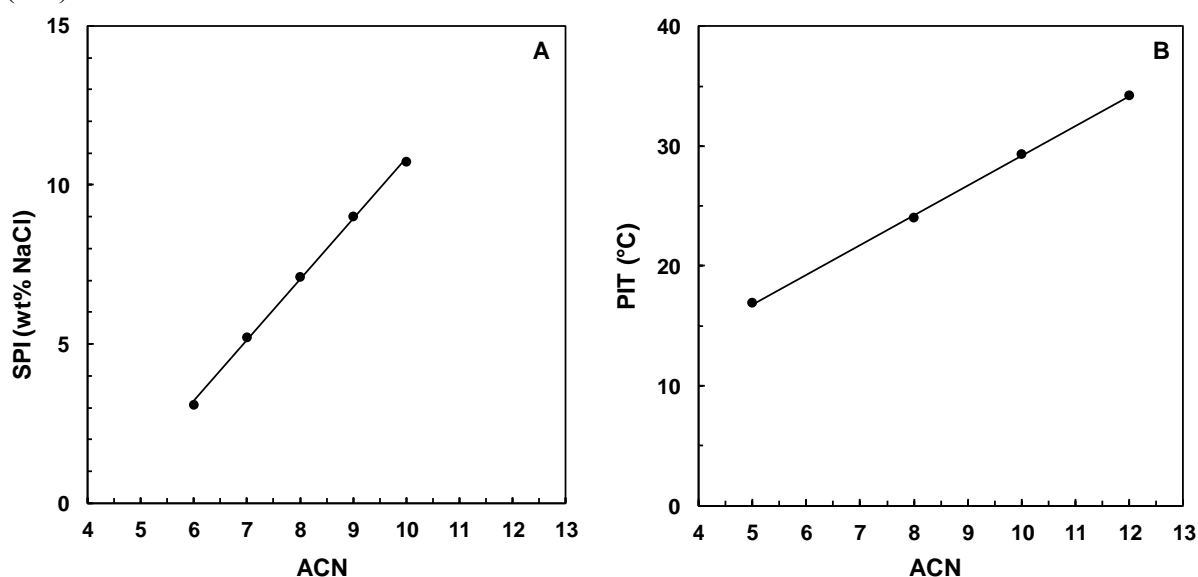

Fig. 6 Evolution of the SPI and the PIT of the C$_{10}$E$_4$ / n-Alkane / Water systems at fw = 0.5 as a function of the number of carbons of the n-alkanes (ACN). A: SPI determined at 15.0 °C B: PIT determined by adjusting the temperature of almost salt-free (0.06 wt% NaCl) SOW systems.

Note that when the carbon number of the n-alkanes (ACN) decreases, the optimal salinity (SPI) and the optimal temperature (PIT) decrease. This behaviour is attributed to the greater or lesser penetration of the n-alkanes within the hydrophobic region of the interfacial film (see Scheme 1). The shorter n-alkanes are more penetrating than the long alkanes and induce a stronger curvature of the interfacial film towards water [38]. Consequently, to restore the optimal formulation (i.e. the zero mean curvature), it is necessary to increase the surface occupied by the polar head of C$_{10}$E$_4$ by increasing the hydrophilicity of its poly(ethylene glycol) chain. This can be achieved by lowering either the temperature of the SOW system or the salinity of the aqueous phase. In addition, it has been shown experimentally that the optimum temperature (T* or PIT) increases linearly when the ACN value of the n-alkane increases [14]. Likewise, Figure 6A shows that optimal salinity (SPI) also increases linearly with ACN in agreement with the HLD$_N$ (Eq. 7). The slope values of the regression lines provide the salt- and thermal- sensitivity parameters: τ$_{C10E4}$ = 0.40 °C^{-1} and δ$_{C10E4}$ = 0.52 wt%$^{-1}$ as well as PACN$_{C10E4}$ = 8.3. The PACN and τ values are consistent with the values calculated from

the known coefficients c_T and k ($\tau_{C10E4} = c_T/k \approx 0.40 \, °C^{-1}$) [35] or from the accurate fish-tail temperatures ($\tau_{C10E4} = 0.38 \, °C^{-1}$, $PACN_{C10E4} = 8.1$) [14]. On the other hand, the experimentally determined δ parameter is substantially lower than that calculated from the coefficients b and k determined 40 years ago by Bourrel et al. using the complex SOW system, ethoxylated nonylphenol / i-pentanol / sec-butanol / n-alcane / $NaCl_{aq}$ ($\delta_{C10E4} \approx b/k = 0.87 \, wt\%^{-1}$) [13,35]. This discrepancy is probably due to the complexity of the SOW system and the technical grade quality of the surfactants used to determine b and k coefficients, whereas in this work, highly pure (> 98%) C_iE_j surfactants and n-alkanes are used. To support this interpretation, let us point out that b and k values have been redetermined more recently by Acosta's group [47] using industrial grade polyethoxylated alcohols C_iE_j. The values of b and k thus obtained vary significantly from one surfactant to another and provide δ values between 0.59 and 0.92. We believe that these wide fluctuations result from the oligomeric nature of industrial surfactants which causes partitioning phenomena of the less ethoxylated oligomers (*vide infra*).

A simpler but less accurate way to obtain the salinity coefficient δ_2 is to apply the HLD equation (7) to the experimental SPI_2 values of the S_2 / n-Octane / Water systems. To use this method, SPI_2 must be within the range of experimentally accessible salinity (0 – 26.3 wt% NaCl). Moreover, $PACN_2$ and the temperature coefficient τ_2 of S_2 must be known which is the case for both surfactants $C_{12}E_5$ and $C_{12}E_6$ [14]. The SPIs measured for $C_{12}E_5$ and $C_{12}E_6$ at 20.0°C are 9.0 and 19.1wt.%, respectively. The salinity coefficients δ of $C_{12}E_5$ and $C_{12}E_6$ were thus calculated and reported in Table 3. The values obtained are close to those determined above for $C_{10}E_4$, confirming the commonly accepted idea that, at least for the $C_{10}E_j$ and $C_{12}E_j$ series, the salinity coefficients δ and the temperature coefficients τ vary little as a function of i and j. Unfortunately, this method is inapplicable to $C_{12}E_7$ and $C_{12}E_8$ because their SPI_2 are above the solubility limit of NaCl in water, nor to $C_{12}E_3$ and $C_{12}E_4$ because their SPI_2 are below 0.

Table 3. Comparison of the SPI-slopes of C_iE_j surfactants measured herein or calculated from Eq. 16 (additive model) by using $PACN_2$ values previously determined by the "fish-tail method" [14] assuming that $PACN_1 = 8.3$ and $\delta_1 = 0.52 \, wt\%^{-1}$. Thermal (τ) and salinity (δ) coefficients are indicated for each surfactant when available.

Surfactant	$PACN^a$	τ^a / $°C^{-1}$	δ / $\%NaCl^{-1}$	SPI-slope / wt% NaCl	
				Measured	Additive model
C_8E_5	-2.4 ± 1.0	0.28	-	21.3 ± 0.6	21 ± 2
$C_{10}E_4$	$8.3 ± 0.2^b$	0.40^b	0.52^b	0	0
$C_{10}E_4$	$8.1 ± 0.2^b$	0.36	-	0	0
$C_{10}E_5$	1.3 ± 0.4	0.34	-	15.0 ± 0.4	13.5 ± 1
$C_{12}E_3$	18 ± 1.0	-	-	-20.5 ± 0.9	-19 ± 1
$C_{12}E_4$	11.8 ± 0.2	0.33	-	-7.2 ± 0.5	-6.7 ± 0.5
$C_{12}E_5$	5.4 ± 0.4	0.36	0.49^c	7.2 ± 0.3	6.0 ± 1
$C_{12}E_6$	-0.5 ± 1.0	0.36	0.54^c	22.6 ± 0.7	17 ± 2
$C_{12}E_7$	-4.7 ± 2.0	0.35	-	38.0 ± 1.2	25 ± 4
$C_{12}E_8$	-9.5 ± 3.0	0.35	-	51.9 ± 2.0	34 ± 6

[a]: Determined from the fish-tail temperatures [14].

[b]: Determined in this work from the PIT and the SPI of $C_{10}E_4$ / n-Alkanes / Water systems (Fig. 6)

[c]: Determined in this work from the SPI of $C_{10}E_4$ / n-Octane / Water systems applied to Eq. (7)

"Additive" model for the SPI_{mix} of mixtures of nonionics

When a surfactant S_2 is added to the $C_{10}E_4$ / *n*-Octane / Water reference system, the resulting HLD is equal to the sum of the HLD_N of the surfactants *present in the interfacial film. If it is further assumed*

that all the surfactants introduced into the system localize within the interfacial film and do not interact together (additive assumption) the total $HLD_{N,mix}$ is then equal to the sum of the HLDs of $C_{10}E_4$ (noted S_1) and S_2, multiplied by their respective molar fractions (Eq. 8).

$$HLD_{N,mix} = HLD_{N,1}.(1 - x_2) + HLD_{N,2}.x_2 = 0 \tag{8}$$

where $HLD_{N,1}$ and $HLD_{N,2}$ represent the respective contributions of $C_{10}E_4$ (Eq. 9) and S_2 (Eq. 10) to the total HLD_N.

$$HLD_{N,1} = PACN_1 - ACN + \delta_1 S + \tau_1(T - 25) \tag{9}$$

$$HLD_{N,2} = PACN_2 - ACN + \delta_2 S + \tau_2(T - 25) \tag{10}$$

According to the protocol used to determine the SPI-slope, the oil is *n*-octane (ACN = 8.0), the temperature is kept constant ($T = T^{SPI} = 20.0\,°C$) and the system ($C_{10}E_4$ + S_2) / *n*-Octane / NaCl$_{aq}$ is at the optimum formulation ($HLD_{N,mix} = 0$). If SPI$_1$ and SPI$_2$ are the optimum salinities measured for the surfactants $C_{10}E_4$ and S_2 alone, it is shown in the Supplementary Material that the SPI of the mixture, $SPI_{mix}(x_2)$, can be expressed according to Eq. 11 as a function of SPI$_1$ and SPI$_2$.

$$SPI_{mix}(x_2) = \frac{SPI_1 - x_2\left(SPI_1 - \frac{\delta_2}{\delta_1}SPI_2\right)}{1 + x_2\left(\frac{\delta_2}{\delta_1} - 1\right)} \tag{11}$$

Analysis of eq. 11, shows that this hyperbolic variation of SPI$_{mix}$(x$_2$) will appear linear when the denominator is negligible. This occurs in two cases: either when the salt-sensitivity coefficients of $C_{10}E_4$ and S_2 are similar ($\delta_1 \approx \delta_2$) or when the concentration x$_2$ of the added surfactant S_2 is much below 1. As the salinity coefficients of $C_{12}E_5$ and $C_{12}E_6$ are close to that of $C_{10}E_4$, the evolution of their SPI$_{mix}$ calculated by applying Eq. (11) should be quasi-linear over the entire range of variation of x$_2$ [0 to 1] (continuous line in Figure 7). Note however that the experimental points are located slightly above the dotted curve corresponding to the additive model (Eq. 11).
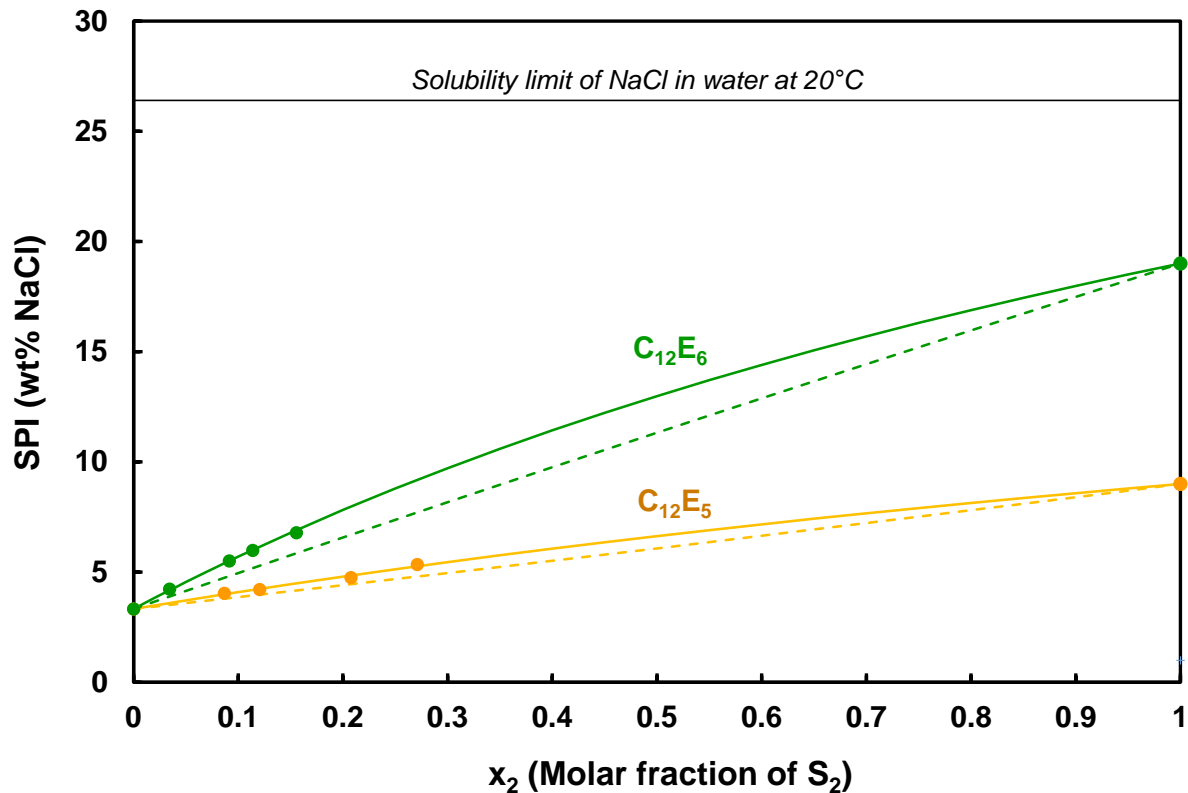
Fig. 7. Evolution of the SPI_{mix} for the systems ($C_{10}E_4 + C_{12}E_5$ or $C_{12}E_6$) / n-Octane / Water at 20°C, f_w = 0.5 and 6 wt% of surfactant, over the entire range of variation of x_2 [0 to 1]. The dotted curves are calculated using the additive model (Eq. 11) and the δ values reported in Table 3. The solid curves correspond to a hyperbolic fitting of the experimental points to take into account the non-additive coefficients γ_1 and γ_2 (Eq. 18).

Under the additive hypothesis, the "additive" SPI-slope noted (SPI-slope)$_{add}$ is, by definition, equal to the derivative of $SPI_{mix}(x_2)$, when x_2 tends towards 0 (i.e. at infinite dilution of surfactant S_2). Under these conditions, the (SPI-slope)$_{add}$ can be expressed as Eq. (12).

$$(SPI\text{-}slope)_{add} = \frac{dSPI_{mix}}{dx_2}\bigg|_{x_2=0} = \frac{\delta_2}{\delta_1}(SPI_2 - SPI_1) \tag{12}$$

However, in most cases the SPI_2 value of surfactant S_2 is not known and it is preferable to replace SPI_1 and SPI_2 by their expressions (13) and (14) giving equation (15) *which is valid for any nonionic surfactant under the additivity hypothesis* (See Supplementary Material for details).

$$SPI_1 = -[PACN_1 - ACN + \tau_1(T^{SPI} - 25)]/\delta_1 \tag{13}$$

$$SPI_2 = -[PACN_2 - ACN + \tau_2(T^{SPI} - 25)]/\delta_2 \tag{14}$$

$$(SPI\text{-}slope)_{add} = \frac{PACN_1 - PACN_2}{\delta_1} + \frac{\tau_1}{\delta_1}\left(\frac{\delta_2}{\delta_1} - \frac{\tau_2}{\tau_1}\right)(T^{SPI} - 25) + \left(\frac{\delta_2}{\delta_1} - 1\right)\frac{PACN_1 - ACN}{\delta_1} \tag{15}$$

It should be noted that under the experimental conditions used to determine the SPI-slope, $S_1 = C_{10}E_4$, oil = *n*-octane and T^{SPI} = 20.0 °C. Therefore, $PACN_1 \approx ACN$ and the third member of the equation is negligible whatever the nonionic surfactant S_2 under study.

Specific case of C_iE_j surfactants

It is commonly admitted that the salt- and the thermal- sensitivity coefficients δ and τ are almost similar for all C_iE_j surfactants [14,35] i.e., $\delta_2 \approx \delta_1$ and $\tau_2 \approx \tau_1$. However, this invariance of the δ and τ parameters is questionable because it seems unlikely that a short surfactant such as C_8E_3 has exactly the same salt and temperature sensitivity as a larger one with a longer chain and many ethoxy units such as $C_{12}E_8$. For example, the Table 3 shows that the value of τ_{C8E5} = 0.28 °C^{-1} varies significantly from the thermal coefficients of the surfactants with C_{10} and C_{12} chains ($\tau_{CiEj} \approx 0.36$ °C^{-1}). Nevertheless, it is reasonable to admit that the sensitivity to salt and temperature of C_iE_j surfactants evolve similarly when the hydrophobic tail C_i and/or the hydrophilic head E_j vary. If this assumption is correct, $\delta_2/\delta_1 \approx \tau_2/\tau_1$ and the second term of the equation (15) also vanishes. So, as a first approximation, the "additive" SPI-slope of C_iE_j surfactants can then be simply expressed as a function of the difference between the $PACN_2$ of S_2 and the $PACN_1$ of the reference surfactant, $C_{10}E_4$ (Eq. 16).

$$(SPI\text{-}slope)_{add} \approx \frac{(PACN_1 - PACN_2)}{\delta_1} \tag{16}$$

Since the $PACN_2$ values of common C_iE_j surfactants were previously determined by the "fish-tail method" [14], the "additive" SPI-slopes of C_iE_j were calculated from Eq. 16 and were compared to the experimental values in Table 3. This table shows that the SPI-slopes thus calculated are either almost equal (C_8E_5, $C_{10}E_5$, $C_{12}E_3$, $C_{12}E_4$, $C_{12}E_5$) or significantly lower ($C_{12}E_6$, $C_{12}E_7$, $C_{12}E_8$) than the experimental values and the difference between them is all the greater as the hydrophilicity of the surfactants S_2 increases. The deviations could either come from the partitioning of $C_{10}E_4$ and S_2 between

the interfacial film, the oil domain and the aqueous domain or from a violation of the $\delta_2/\delta_1 \approx \tau_2/\tau_1$ hypothesis.

4.2 Model considering the partitioning of $C_{10}E_4$ and S_2 in the oil and aqueous phases

As noted above, the SPI-slopes of nonionic surfactants $C_{12}E_6$, $C_{12}E_7$, $C_{12}E_8$ are higher than expected whereas the SPI-slope of the ionic surfactant C_8NMe_3Br is lower than expected. These observations strongly suggest that $C_{10}E_4$ and/or S_2 surfactants introduced into the medium are not solely located in the interfacial film but undergo a thermodynamic partitioning between the interface, the oil domain and the aqueous domain as shown in Scheme 1 [39–43]. The partitioning phenomenon is well documented for mixtures of oligomeric polyethoxylated surfactants whose partition coefficients between the aqueous, the oil and the microemulsion phases depend on the number of ethoxy groups and vary with temperature [6,44]. As temperature increases, the less hydrophilic oligomers tend to migrate into the oil while the more hydrophilic ones remain at the interface. As a result, the composition of the interfacial film, which governs the phase inversion, is depleted in hydrophobic oligomers and appears more hydrophilic than expected.

Contrariwise when S_2 is a short and very hydrophilic ionic surfactant, the partitioning phenomenon also occurs except that, in this case, the ionic surfactant migrates into the aqueous phase since it exhibits a high monomolecular solubility in water. For instance, Figure 5B shows that C_8NMe_3Br substantially deviates from the monotonous behaviour observed for the other members of the series. Here, the explanation mirrors that for nonionic surfactants. Indeed, a significant fraction of this added surfactant S_2 partitions into water instead of being located in the interfacial film next to $C_{10}E_4$. As a consequence, the mixed interfacial film ($C_{10}E_4 + S_2$) is less hydrophilic and the measured SPI-slope is lower than anticipated. As explained in the previous publications dedicated to the PIT-slope method, the partitioning phenomenon also occurs even more dramatically (compare 5B and 5 D) when temperature is modified rather than salinity and also induces an underestimation of the PIT-slopes for short chain amphiphiles [17].

Accordingly, the simplifying hypothesis that surfactants $C_{10}E_4$ and S_2 introduced in solution are essentially localized at the interface is no longer verified when one of the surfactants, or both, partially migrate towards the aqueous or oil phase. These migrations depend on the intrinsic hydrophilic/lipophilic ratios (PACN) of the surfactants $C_{10}E_4$ and S_2 but also on the polarity of the oil. To account for the partitioning of the surfactants and any other phenomenon prone to disturb the simple additivity rule of HLD_N, equation (8) must be generalized by introducing "non-additivity coefficients" γ_i which modulate the contributions of $C_{10}E_4$ and S_2 to HLD_N (Eq. 17).

$$HLD_{N,mixture} = HLD_{N,1} . \gamma_1 (1 - x_2) + HLD_{N,2} . \gamma_2 x_2 = 0 \qquad (17)$$

The most likely causes of γ_1 or $\gamma_2 \neq 1$ are either that one or both surfactants significantly migrate into the aqueous or oil phase (*i.e.* full adsorption at the interface assumption is violated), or that interactions between surfactants $C_{10}E_4$ and S_2 at the interface modify the effective $HLD_{N,2}$ of S_2. The influence of these "non-additivity" coefficients γ_i will be discussed both on the SPI-slope and on the PIT-slope because a comparison of these two parameters will be carried out in the section 4.3.

The coefficients γ_1 and γ_2 can be interpreted as follows.

- *Depletion of the reference surfactant $C_{10}E_4$ from interface ($\gamma_2/\gamma_1 > 1$)*

During the SPI-slope (and the PIT slope) experiments, a non-negligible part of $C_{10}E_4$ is dissolved as

monomers in the oil phase and this proportion increases with temperature [26]. This partitioning contradicts the full adsorption assumption and decrease the contribution of $HLD_{N,1}$ with respect to $HLD_{N,2}$ in Eq. (17). In this case, $\gamma_2/\gamma_1 > 1$ and the measured SPI-slope (and the PIT slope) is higher than expected if the additivity assumption was valid. (See Figure 7)

- *Depletion of the studied surfactant S_2 from interface ($\gamma_2/\gamma_1 < 1$)*

When the surfactant S_2 has a high CMC in water, (like ionic surfactants with short alkyl chains), the monomeric form of S_2 will be present in significant amounts within the aqueous compartments during the SPI- and the PIT-slope experiments leading to $\gamma_2/\gamma_1 < 1$. Therefore, the contribution $HLD_{N,1}$ of the reference surfactant $C_{10}E_4$ to $HLD_{N,mix}$ will be favoured with respect to surfactant S_2 and the measured SPI-slope (and the PIT slope) will be lower than expected from the additivity assumption (See Figure 5B and 5D).

- *Favourable interactions of S_2 with C_{10}E_4 ($\gamma_2 < 1$)*

Favourable headgroup interactions between an ionic surfactant S_2 and $C_{10}E_4$ (Scheme 1) would decrease the apparent hydrophilicity of S_2 and would reduce the magnitude of apparent $HLD_{N,2}$.

When the ratio γ_2/γ_1 is substantially greater or less than one, equation (11) describing the evolution of SPI_{mix} becomes equation (18) which integrates the non-additivity terms (see Supplementary Material

for the demonstration).

$$SPI_{mix}(x_2) = \frac{SPI_1 - x_2\left(SPI_1 - \frac{\gamma_2\delta_2}{\gamma_1\delta_1}SPI_2\right)}{1 + x_2\left(\frac{\gamma_2\delta_2}{\gamma_1\delta_1} - 1\right)} \tag{18}$$

Consequently, even when $\delta_1 \approx \delta_2$, the denominator of equation (18) is no longer negligible and the evolution of SPI_{mix} is an arc of hyperbola as shown in Figure 7 (solid curves) for the surfactants $C_{12}E_5$ and $C_{12}E_6$. The fact that the experimental points are slightly above the "additive" dotted line shows that the ratio γ_2/γ_1 is higher than the unity. However, the curvature of the hyperbola is small enough at the beginning of the curve so that experimental points used for determining the SPI-slope can be correctly approximated by the tangent at the origin expressed by equation (19).

$$(SPI\text{-}slope) = \frac{\gamma_2}{\gamma_1}(SPI\text{-}slope)_{add} \tag{19}$$

By comparing the slope of the tangent at the origin (SPI-slope) and that of the line corresponding to the additive model (SPI-slope)$_{add}$, we find that γ_2/γ_1 is equal to 1.3 for $C_{12}E_5$ and 1.4 for $C_{12}E_6$. These deviations from linearity are largely due to the migration of a significant part of $C_{10}E_4$ into n-octane. According to the partitioning of $C_{10}E_4$ measured by Pizzino et al. for the $C_{10}E_4$ / n-Octane / Water system [26] and knowing the CMC of $C_{10}E_4$ in water (0.64 mM) [37], the partitioning of $C_{10}E_4$ can be estimated at T^{SPI} (20 °C). Thus, the aqueous phase contains 0.3% of the added $C_{10}E_4$, the n-octane phase, 21.5% and the interfacial film, 78.2%. Considering this thermal partitioning of $C_{10}E_4$ in n-octane as the only source of deviation, γ_2/γ_1 should be equal to 1.3 for very hydrophilic $C_{10}E_4$ surfactants. However, surfactants having a PACN close to that of $C_{10}E_4$ will also undergo significant partitioning towards n-octane leading to a decrease of γ_2 and a γ_2/γ_1 ratio ≈ 1.

4.3 2D-Mapping of the test surfactants S_2 according to their PIT-slope and SPI-slope

In summary, the PIT-slope quantitatively expresses the hydrophilic-lipophilic ratio of the test surfactant

S_2 at low salinity (0.06 wt%) while the SPI-slope accounts for the same ratio but at high salinity (> 1 wt%). It is important to note that the phase inversion used here to detect the optimum formulation *is triggered only when the HLD$_N$ value of the surfactants present at the O/W interface is zero.* However, as discussed in the previous paragraph, the composition of the interfacial film may differ significantly from the $C_{10}E_4/S_2$ mixture introduced into the medium, particularly at higher temperature that enhances the migration of $C_{10}E_4$ towards the oil domain.

The PIT- and SPI-slopes are defined mathematically as the derivatives at the origin, *i.e.* when x_2 tends towards 0, of the PIT and SPI curves as a function of x_2. In order for the measured slopes to be strictly in accordance with the derivatives at the origin, the added amount of S_2 should be infinitesimal as well as the changes in temperature or salt concentration required to restore the optimal formulation. However, to experimentally determine these slopes with good precision, it is necessary to modify the temperature between 15 and 40 °C [17] and the salinity between 1 and 10 wt% depending on whether S_2 is much less, or much more, hydrophilic than $C_{10}E_4$ (See Figure 3). As discussed above, in these temperature and salinity ranges, a non-negligible part of $C_{10}E_4$ lies in the oil phase and its proportion increases with the temperature leading to a significant overestimation of the PIT-slope for very hydrophilic S_2 surfactants compared to the value that would be obtained if all the surfactants $C_{10}E_4$ and S_2 would remain confined at the O/W interface. This partitioning phenomenon will mainly expand the PIT-slope scale but much less the SPI-slope scale because the measurements are carried out at constant temperature (20.0 °C). However, stretching the scales will not modify the actual order of the hydrophilic-lipophilic ratios of the surfactants. As the two methods provide complementary information regarding the salt-sensitivity and the thermal-sensitivity of surfactants, it is tempting to position on a 2D map all the surfactants S_2 tested according to their PIT-slope and their SPI-slope values (Figure 8). This graphical presentation facilitates the comparison of the hydrophilic-lipophilic-ratios and the salt-sensitivities of the surfactants polar heads and highlight the evolution of the PIT-slope and SPI-slope for homologous series of surfactants.
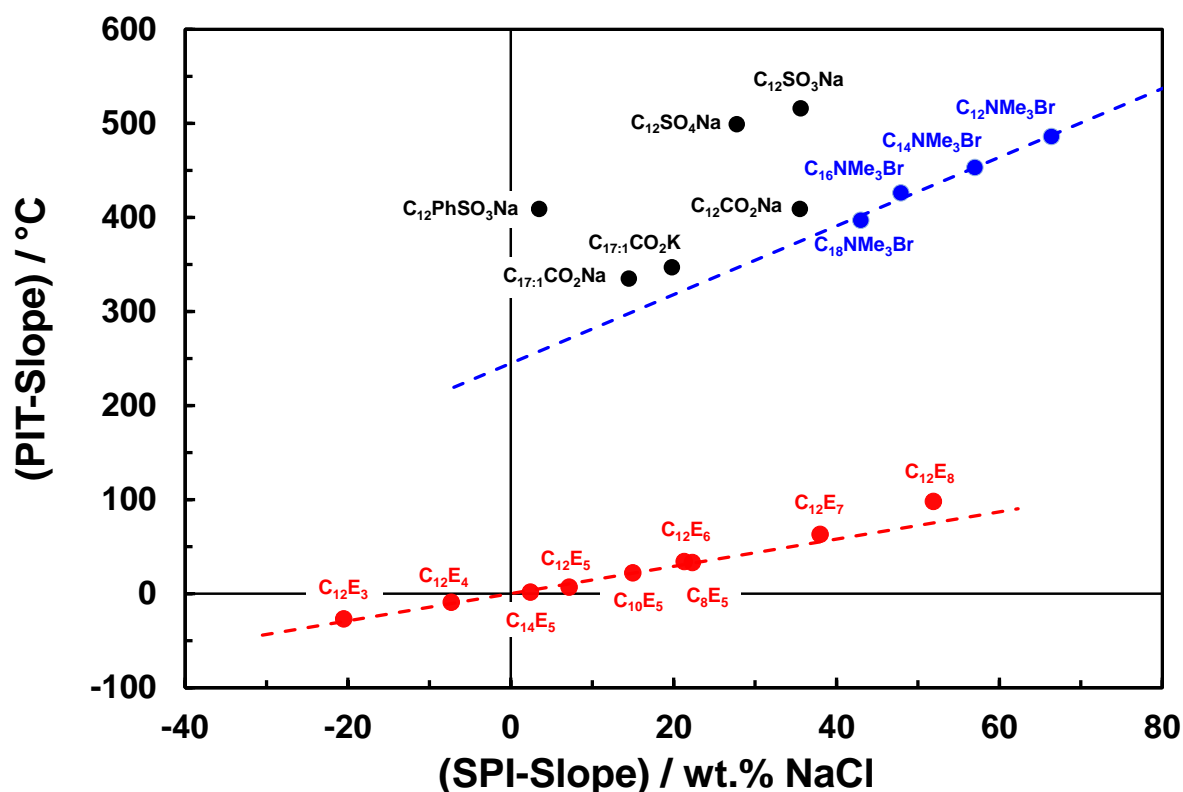

Fig. 8. 2D experimental map of surfactants S_2 positioned according to their measured PIT-slope and

SPI-slope values. Dotted lines correspond to the observed tendencies for homologous series of surfactants.

4.3.1. Qualitative discussion

A simple observation of the location of surfactants with C_{12} chains in Figure 8 provides some relevant information on the hydrophilicity and the salt sensitivity of the different polar heads. First, ionic surfactants are all much above nonionics in agreement with their greater hydrophilicity in salt-free media i.e., PACN (ionic surfactants) << PACN (nonionic surfactants). More specifically, at low salinity (0.06 wt% NaCl) corresponding to the PIT-slope conditions, the sulfonate function appears slightly more hydrophilic than the sulphate and tetramethyl ammonium functions and significantly more hydrophilic than the carboxylate function whereas, at high salinity (> 3 wt% NaCl) corresponding to SPI-slope conditions, the order of apparent hydrophilicity is completely upset as shown in Figures 4 and 8. Only the ionic surfactant with a quaternary ammonium head group and a C_{12} chain appears to be more hydrophilic than $C_{12}E_7$ and $C_{12}E_8$, while the other ionic functions see their apparent hydrophilicity considerably reduced. This observation agrees with the much higher salt-tolerance of nonionics compared to ionics. Further, the sodium sulphate and sulfonate polar heads appear to be more subject to the charge screening phenomenon by NaCl than the quaternary ammonium bromide head group. Another interesting remark concerns the homologous series of ionic C_nNMe_3Br and nonionic $C_{12}E_j$ surfactants which are aligned, except $C_{10}N(Me)_3Br$ and, to a much lesser extent, $C_{12}E_7$ and $C_{12}E_8$. Moreover, we see that all other C_iE_j, whatever the chain length and the number of ethoxylates, are located on the same straight line which passes through the origin. All these observations are rationalized below on the basis of the HLD_N equations (8) and (17).

4.3.2. Quantitative assessment

Assuming the additive HLD_N model (Eq. 8), the PIT-slope of the test surfactant S_2 can be expressed according to equation (20) as a function of the characteristic parameters of the surfactants $C_{10}E_4$ (S_1) and S_2 (see Supplementary Material for details).

$$(PIT\text{-}slope)_{add} = \frac{PACN_1 - PACN_2}{\tau_1} + \frac{\delta_1}{\tau_1}\left(\frac{\tau_2}{\tau_1} - \frac{\delta_2}{\delta_1}\right)S^{PIT} + \left(\frac{\tau_2}{\tau_1} - 1\right)\frac{PACN_1 - ACN}{\tau_1} \quad (20)$$

Where ACN (= 8.0) and S^{PIT} (= 0.06 wt% NaCl) correspond to the oil (*n*-octane) and the salinity used to determine the PIT-slopes while the characteristic parameters of S_1 and S_2 namely $PACN_1$, $PACN_2$, δ_1, δ_2, τ_1 and τ_2 have their usual meanings.

By eliminating the term ($PACN_1$ - $PACN_2$) between equations (15) and (20), the linear relationship (21) between the PIT-slope and the SPI-slope is obtained.

$$(PIT\text{-}slope)_{add} = \frac{\delta_1}{\tau_1}(SPI\text{-}slope)_{add} + \left(\frac{\delta_2}{\delta_1} - \frac{\tau_2}{\tau_1}\right)\left(-\frac{PACN_1 - ACN + \delta_1 S^{PIT}}{\tau_1} - 25 - T^{SPI}\right) \quad (21)$$

Considering the expression (22) of the phase inversion temperature PIT_1 of $C_{10}E_4$ alone as a function of its characteristic parameters, the more compact equation (23) can be derived from equation (20).

$$PIT_1 = 25 - \frac{PACN_1 - ACN + \delta_1 S^{PIT}}{\tau_1} \quad (22)$$

$$(PIT\text{-}slope)_{add} = \frac{\delta_1}{\tau_1}(SPI\text{-}slope)_{add} + \left(\frac{\delta_2}{\delta_1} - \frac{\tau_2}{\tau_1}\right)(PIT_1 - T^{SPI}) \quad (23)$$

By replacing the known constant parameters (δ_1, τ_1, PIT_1, T^{SPI}, S^{PIT}) by their numerical values (0.52

wt%$^{-1}$, 0.40 °C^{-1}, 23.9°C, 20.0 °C, 0.06 wt%), one obtains the simpler relation (24), *valid for any nonionic surfactants in the framework of the "additive" model (Eq. 8).*

$$(PIT\text{-}slope)_{add} \approx 1.3 \, (SPI\text{-}slope)_{add} + 7.5 \, \delta_2 - 9.8 \, \tau_2 \tag{24}$$

Furthermore, in the specific case of C_iE_j surfactants, it can be assumed that $\delta_2/\delta_1 \approx \tau_2/\tau_1$. Supposing this simplifying hypothesis, the 2nd term of Eq. (23) should also vanishes leading to Eq. (25) which predicts that all representative points of C_iE_j surfactants should fall on a straight line with no intercept and with a slope of about 1.3 °C/wt%.

$$(PIT\text{-}slope)_{add} = \frac{\delta_1}{\tau_1} \, (SPI\text{-}slope)_{add} = 1.3 \, (SPI\text{-}slope)_{add} \tag{25}$$

Table 4 and Figure 9 focused on C_iE_j surfactants shows that the relation (25) is reasonably verified for the surfactants having a hydrophilic/lipophilic ratio close to that of $C_{10}E_4$ but that the more their hydrophilicity increases, the more they are located above from the straight line.
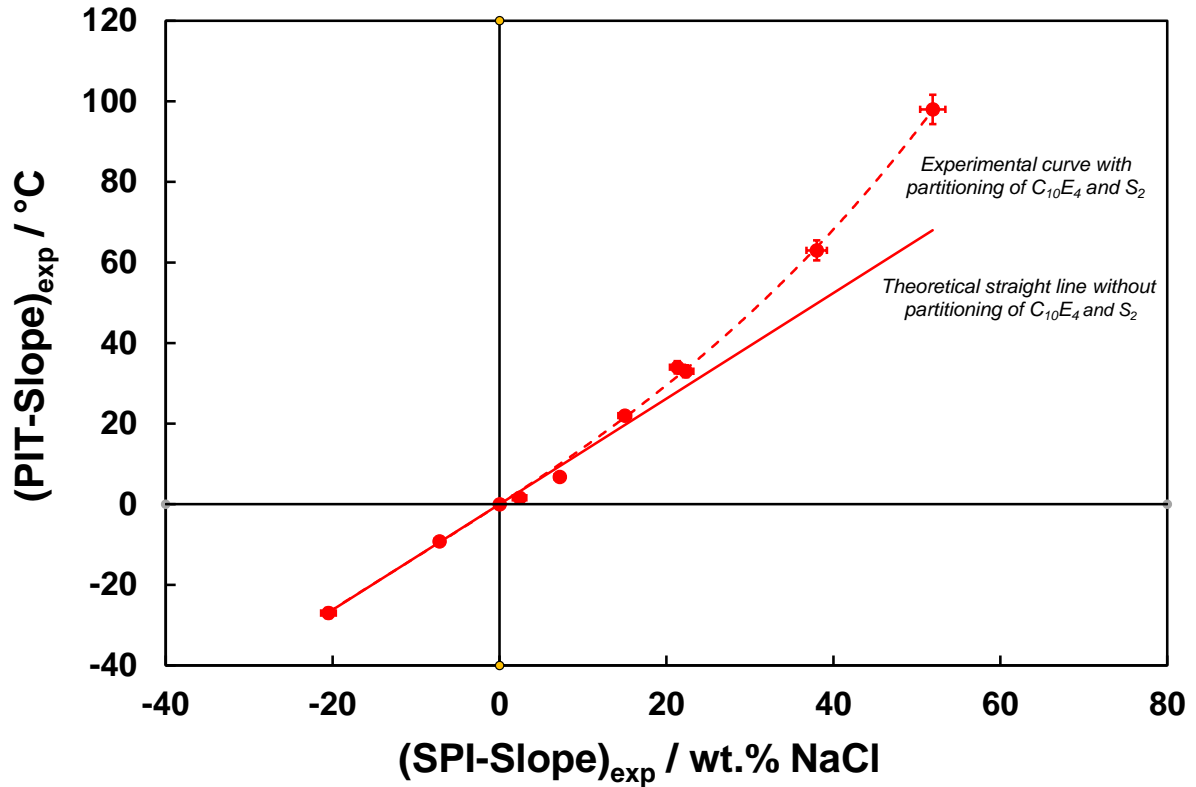

Fig. 9. PIT-slope vs SPI-slope map of C_iE_j surfactants. The straight line corresponds to the equation (25) predicted by the "additive" model and the dotted curve to the evolution observed experimentally.

Table 4. Ratio between the PIT-slope and the SPI-slope of C_iE_j surfactants ordered by increasing hydrophilicity.

Surfactant	SPI-slope / wt% NaCl	PIT-slope / °C	PIT-slope / SPI-slope
$C_{12}E_3$	-20.5 ± 0.9	-27.0 ± 1.3	1.3 ± 0.1
$C_{12}E_4$	-7.2 ± 0.5	-9.2 ± 0.7	1.3 ± 0.2
$C_{10}E_4$	0	0	-
$C_{14}E_5$	2.4 ± 0.8	1.6 ± 0.9	0.7 ± 0.7
$C_{12}E_5$	7.2 ± 0.3	6.8 ± 0.6	0.9 ± 0.2

Surfactant	SPI-slope / wt% NaCl	PIT-slope / °C	PIT-slope / SPI-slope
$C_{10}E_5$	15.0 ± 0.4	22.0 ± 1.1	1.5 ± 0.2
$C_{12}E_6$	22.6 ± 0.7	33 ± 1.5	1.5 ± 0.1
C_8E_5	21.3 ± 0.6	34 ± 1.5	1.6 ± 0.1
$C_{12}E_7$	38.0 ± 1.2	63 ± 2.5	1.7 ± 0.1
$C_{12}E_8$	51.9 ± 2.0	98 ± 3.6	1.9 ± 0.1

We assume that thermal partitioning of $C_{10}E_4$ in favour of the oil phase is the main cause of this deviation. It is important to emphasize that the thermal partitioning of $C_{10}E_4$ affects differently the PIT-slope and the SPI-slope. In the PIT-slope, when adding a very hydrophilic surfactant such as $C_{12}E_8$ to the SOW reference system, the PIT increases gradually and the monomeric solubility of the $C_{10}E_4$ in the oily phase also does. In contrast, in the SPI-slope, T^{SPI} (20.0°C) is significantly lower than T^{PIT} (25.0°C) and the monomeric solubilization in n-octane is thus lower from the start [26]. Moreover, the temperature is maintained constant at 20.0°C throughout the whole measurement and so is the monomeric solubility of $C_{10}E_4$ in n-octane. Consequently, the SPI-slope scale only undergoes a slight "stretching effect" while for the PIT-slope scale, the stretching is much stronger. The more hydrophilic the surfactant, the more the measured PIT-slope will be overestimated compared to the value which would be obtained if $C_{10}E_4$ remained located at the interface. This phenomenon is particularly significant for ionic surfactants which are considerably more hydrophilic than nonionic surfactants in a low-salt environment (PIT-slope conditions). However, the available data are insufficient to quantitatively model these stretching effects and are, anyway, well outside the scope of this article which is mainly dedicated to the description of the SPI-slope method.

5   Conclusion

The sensitivity of surfactants to electrolytes is an important theoretical and practical issue as the interactions between surfactants and electrolytes play a key role in a number of significant industrial processes. Among these we can mention, the tolerance of detergents towards hard water, the obtainment of ultra-low interfacial tension for EOR or the viscosification of shampoos by adding salt to form giant micelles. The usual method for evaluating the salt effect on a surfactant consists in constructing its binary phase diagram in water (temperature vs salt) by plotting the incipient phase separations (cloud and/or Krafft points) [45]. This strategy is time consuming and is only applicable to water-soluble surfactants. A more versatile method, based on the optimum formulation was proposed recently by Zarate *et al* [46]. They start from the nonionic reference system $C_{8-10}E_{4.5}$ / Hexane / Water to which variable amounts of S_2 is added. For each concentration of S_2 a series of vials with different salt concentration is prepared and the optimal salinity S* is determined visually by detecting the vials with the least stable emulsion. Finally, S* values are plotted as a function of the molar fraction x_2 of the S_2 in order to determine $PACN_2$ (named Characteristic curvature Cc in their paper). The SPI-slope method presented here is related to the previous ones but is even closer to the PIT-slope method [17]. Actually, in our case, *the reference surfactant $C_{10}E_4$ is pure (> 99 %), the salinity scan is continuous and the optimal salinity is precisely detected by a sudden drop (or increase) in conductivity*. As a result, detecting the optimal salinity is faster, more accurate and more reproducible than discontinuous methods using technical grade surfactants.

The optimal salinity causing phase inversion (SPI) of the reference system ($C_{10}E_4$ 3 wt%) / n-Octane / $NaCl_{aq}$ varies linearly with the molar fraction x_2 when increasing amounts of S_2 is added. This linear

variation is quantified by the slope dSPI/dx$_2$, called "SPI-slope", which is expressed in wt% of NaCl. A positive (or negative) SPI-slope is obtained when the salinity needed to invert the emulsion is higher (or lower) than for the neat reference system. For surfactants with the same dodecyl tail, the SPI-slope method allows determining the effective hydrophilicity of a series of ionic and nonionic polar heads *in saline environment:* $C_{12}NMe_3Br > C_{12}E_8 > C_{12}E_7 \approx C_{12}SO_3Na \approx C_{12}CO_2Na > C_{12}SO_4Na > C_{12}E_6 > C_{12}E_5 > C_{12}E_3$. This order is quite similar to the one obtained by Bourrel [34] using a salinity scan with samples at equilibrium, indicating that for a given PACN, high SPI-slope values are correlated with high salt-tolerances. The nonionic surfactants $C_{12}E_7$ and $C_{12}E_8$ have a higher SPI-slope than $C_{12}SO_4Na$ due to the excellent salt-tolerance of ethoxy groups.

A simple "additive" model, based on the HLD$_N$ equation and neglecting the partitioning of $C_{10}E_4$ and S$_2$, has been developed for all types of nonionic surfactants to express the SPI-slope as a function of the hydrophilic/lipophilic ratio (PACN$_2$) and the salinity coefficient (δ_2) of S$_2$ (Eq. 15). This model, applied to C$_i$E$_j$ surfactants, slightly underestimates the experimental SPI-slopes due to a partial migration of the surfactants $C_{10}E_4$ and S$_2$ in the n-octane phase. The non-additivity effect of *HLD$_N$* on the SPI-slope were formalized by introducing a corrective coefficient γ_i which accounts for the partitioning of $C_{10}E_4$ and/or S$_2$ into the aqueous and/or oil phases and for the possible specific interactions between $C_{10}E_4$ and S$_2$. A similar model could not be developed for the SPI slopes of ionic surfactants. Indeed, according to the HLD$_N$ equations, the influence of salinity is linear for nonionic surfactants and logarithmic for ionic surfactants which makes it impossible to obtain an analytical solution of the SPI-slope as a function of the characteristic coefficients of $C_{10}E_4$ and S$_2$. One way to circumvent this problem would be to replace the reference surfactant $C_{10}E_4$ by an ionic as similar as possible to that studied. Thus, SPI$_{mix}$ would only include terms in LnS and a mathematical expression of the SPI-slope of S$_2$ could be inferred. In addition, the migration of this surfactant towards the oil would be less than with $C_{10}E_4$ but it would increase towards the aqueous phase. Such a ionic reference surfactant has been used by Witthayapanyanon et al. [47] to characterize several anionic extended surfactants by salinity scans using the di-hexyl sodium sulfosuccinate as reference. Interestingly however, the low sensitivity to electrolytes of the current reference surfactant $C_{10}E_4$ makes it well suited for assessing the salt-tolerance of S$_2$ to relevant electrolytes such as calcium salts present in hard water or in oil rocks.

Finally, all studied surfactants have been positioned on a 2D map according to the values of their SPI-slope and PIT-slope. This graphic presentation highlights in a very synthetic and visual way the effective hydrophilic/lipophilic ratios of the surfactants in media salt-free or very salty media. It is therefore a useful tool to help formulators to choose the most appropriate surfactants for a given application [19].

Further research is under way to apply the 2D map PIT-slope / SPI-slope for choosing the most effective technical grade surfactants, especially in the field of Enhanced Oil Recovery (EOR) where the salinity is the preferred formulation variable for identifying the optimal formulation of Surfactant / Crude oil / Brine systems. By replacing NaCl with other electrolytes, the SPI-slope method could also quantitatively estimate the salting-in and salting-out effect of anions and cations on the phase inversion.

SUPPLEMENTARY MATERIAL

Demonstrations of the SPI-slope and PIT-slope equations.

Relationship between PIT-slope and SPI-slope for nonionics

Apparent linearity of the SPI-slope

Expression of the SPI using the parameters of the historical HLD equation

Conductivity vs. Salinity profiles for $C_{10}E_4$, $C_{12}E_5$ and $C_{12}E_6$

Numeric examples of mass balances

Glossary of abbreviations and symbols

REFERENCES

[1] T.F. Tadros, Applied surfactants: principles and applications, John Wiley & Sons, 2006.

[2] W.C. Griffin, Classification of surface-active agents by "HLB," J Soc Cosmet. Chem. 1 (1949) 311–326.

[3] W.C. Griffin, Calculation of HLB values of non-ionic surfactants, J Soc Cosmet Chem. 5 (1954) 249–256.

[4] J.T. Davies, A quantitative kinetic theory of emulsion type, I. Physical chemistry of the emulsifying agent, in: Proc. 2nd Int. Congr. Surf. Act., 1957: p. 426.

[5] J.N. Israelachvili, D.J. Mitchell, B.W. Ninham, Theory of self-assembly of hydrocarbon amphiphiles into micelles and bilayers, J. Chem. Soc. Faraday Trans. 2. 72 (1976) 1525. https://doi.org/10.1039/f29767201525.

[6] J.-L. Salager, N. Marquez, A. Graciaa, J. Lachaise, Partitioning of Ethoxylated Octylphenol Surfactants in Microemulsion−Oil−Water Systems: Influence of Temperature and Relation between Partitioning Coefficient and Physicochemical Formulation, Langmuir. 16 (2000) 5534–5539. https://doi.org/10.1021/la9905517.

[7] J.-L. Salager, A.M. Forgiarini, J. Bullón, How to Attain Ultralow Interfacial Tension and Three-Phase Behavior with Surfactant Formulation for Enhanced Oil Recovery: A Review. Part 1. Optimum Formulation for Simple Surfactant–Oil–Water Ternary Systems, J. Surfactants Deterg. 16 (2013) 449–472. https://doi.org/10.1007/s11743-013-1470-4.

[8] J.-L. Salager, A. Forgiarini, R. Marquez, Extended Surfactants Including an Alkoxylated Central Part Intermediate Producing a Gradual Polarity Transition-A Review of the Properties Used in Applications Such as Enhanced Oil Recovery and Polar Oil Solubilization in Microemulsions, J. Surfactants Deterg. 22 (2019) 935–972. https://doi.org/10.1002/jsde.12331.

[9] J.L. Salager, I. Loaiza-Maldonado, M. Minana-Perez, F. Silva, Surfactant-Oil-Water systems near the affinity inversion Part I: Relationship between equilibrium phase behavior and emulsion type and stability, J. Dispers. Sci. Technol. 3 (1982) 279–292. https://doi.org/10.1080/01932698208943642.

[10] J.-L. Salager, R. Anton, J.-M. Aubry, Formulation des émulsions par la méthode du HLD, Tech. L'Ingénieur. (2006) J2158.

[11] E. Acosta, E. Szekeres, D.A. Sabatini, J.H. Harwell, Net-Average Curvature Model for Solubilization and Supersolubilization in Surfactant Microemulsions, Langmuir. 19 (2003) 186–195. https://doi.org/10.1021/la026168a.

[12] J.L. Salager, J.C. Morgan, R.S. Schechter, W.H. Wade, E. Vasquez, Optimum formulation of surfactant/water/oil systems for minimum interfacial tension or phase behavior, Soc Pet Eng J. 19 (1979) 107–115.

[13] M. Bourrel, J.L. Salager, R.S. Schechter, W.H. Wade, A correlation for phase behavior of nonionic surfactants, J. Colloid Interface Sci. 75 (1980) 451–461.

[14] J.-M. Aubry, J.F. Ontiveros, J.-L. Salager, V. Nardello-Rataj, Use of the normalized hydrophilic-lipophilic-

deviation (HLD_N) equation for determining the equivalent alkane carbon number (EACN) of oils and the preferred alkane carbon number (PACN) of nonionic surfactants by the fish-tail method (FTM), Adv. Colloid Interface Sci. 276 (2020) 102099. https://doi.org/10.1016/j.cis.2019.102099.

[15] J.L. Salager, A Normalized Hydrophilic-Lipophilic-Deviation Expression HLD_N is necessary to avoid confusion close to the optimum formulation of Surfactant-Oil-Water systems, J. Surfactants Deterg. (2021) jsde.12518. https://doi.org/10.1002/jsde.12518.

[16] J.F. Ontiveros, C. Pierlot, M. Catté, V. Molinier, J.-L. Salager, J.-M. Aubry, A simple method to assess the hydrophilic lipophilic balance of food and cosmetic surfactants using the phase inversion temperature of $C_{10}E_4$/n-octane/water emulsions, Colloids Surf. Physicochem. Eng. Asp. 458 (2014) 32–39. https://doi.org/10.1016/j.colsurfa.2014.02.058.

[17] J.F. Ontiveros, C. Pierlot, M. Catté, V. Molinier, J.-L. Salager, J.-M. Aubry, Structure-interfacial properties relationship and quantification of the amphiphilicity of well-defined ionic and non-ionic surfactants using the PIT-slope method, J. Colloid Interface Sci. 448 (2015) 222–230. https://doi.org/10.1016/j.jcis.2015.02.028.

[18] J.F. Ontiveros, C. Pierlot, M. Catté, J.-L. Salager, J.-M. Aubry, Determining the Preferred Alkane Carbon Number (PACN) of nonionic surfactants using the PIT-slope method, Colloids Surf. Physicochem. Eng. Asp. 536 (2018) 30–37. https://doi.org/10.1016/j.colsurfa.2017.08.002.

[19] G. Lemahieu, J.F. Ontiveros, N. Terra Telles Souza, V. Molinier, J.-M. Aubry, Fast and accurate selection of surfactants for enhanced oil recovery by dynamic Salinity-Phase-Inversion (SPI), Fuel. 289 (2021) 119928. https://doi.org/10.1016/j.fuel.2020.119928.

[20] J.L. Salager, M. Miñana-Pérez, M. Perez-Sanchez, M. Ramfrez-Gouveia, C.I. Rojas, Surfactant-oil-water systems near the affinity inversion part III: The two kinds of emulsion inversion, J. Dispers. Sci. Technol. 4 (1983) 313–329.

[21] T. Gibson, Phase-transfer synthesis of monoalkyl ethers of oligoethylene glycols, J. Org. Chem. 45 (1980) 1095–1098.

[22] J.C. Lang, R.D. Morgan, Nonionic surfactant mixtures. I. Phase equilibria in CE–HO and closed-loop coexistence, J. Chem. Phys. 73 (1980) 5849.

[23] J. Schlarmann, C. Stubenrauch, R. Strey, Correlation between film properties and the purity of surfactants, Phys. Chem. Chem. Phys. 5 (2003) 184–191. https://doi.org/10.1039/b208899c.

[24] M. Kahlweit, R. Strey, P. Firman, Search for tricritical points in ternary systems: water-oil-nonionic amphiphile, J. Phys. Chem. 90 (1986) 671–677.

[25] M. Kahlweit, G. Busse, J. Winkler, Electric conductivity in microemulsions, J. Chem. Phys. 99 (1993) 5605–5614. https://doi.org/10.1063/1.465953.

[26] A. Pizzino, V. Molinier, M. Catté, J.-L. Salager, J.-M. Aubry, Bidimensional Analysis of the Phase Behavior of a Well-Defined Surfactant $C_{10}E_4$/n-Octane/Water−Temperature System, J. Phys. Chem. B. 113 (2009) 16142–16150. https://doi.org/10.1021/jp907261u.

[27] M. Kahlweit, R. Strey, D. Haase, J. Jen, General Patterns of the Phase Behavior of Mixtures of H_2O, Nonpolar Solvents, Amphiphiles, and Electrolytes., Langmuir. (1988) 13.

[28] J.L. Salager, R.E. Antón, Physico-chemical characterization of a surfactant a quick and precise method, J. Dispers. Sci. Technol. 4 (1983) 253–273. https://doi.org/10.1080/01932698308943370.

[29] H. Kunieda, Y. Fukui, H. Uchiyama, C. Solans, Spontaneous formation of highly concentrated water-in-oil emulsions (gel-emulsions), Langmuir. 12 (1996) 2136–2140.

[30] B. Heurtault, P. Saulnier, B. Pech, J.-E. Proust, J.-P. Benoit, A novel phase inversion-based process for the preparation of lipid nanocarriers, Pharm. Res. 19 (2002) 875–880.

[31] N. Anton, J.-P. Benoit, P. Saulnier, Particular conductive behaviors of emulsion phase inverting, J. Drug

Deliv. Sci. Technol. 18 (2008) 95–99.

[32]   M. Corti, C. Minero, V. Degiorgio, Cloud point transition in nonionic micellar solutions, J. Phys. Chem. 88 (1984) 309–317.

[33]   M. Kahlweit, E. Lessner, R. Strey, Phase behavior of quaternary systems of the type water-oil-nonionic surfactant-inorganic electrolyte. 2, J. Phys. Chem. 88 (1984) 1937–1944. https://doi.org/10.1021/j150654a005.

[34]   M. Bourrel, R.S. Schechter, Microemulsions and related systems: formulation, solvency, and physical properties, M. Dekker, New York, 1988.

[35]   J.-L. Salager, R.E. Antón, J.M. Anderez, J.-M. Aubry, Formulation des micro-émulsions par la méthode HLD, Tech. L'Ingénieur, (2001) J2157.

[36]   S.-G. Oh, J. Kizling, K. Holmberg, Microemulsions as reaction media for synthesis of sodium decyl sulfonate 2. Role of ionic surfactants, Colloids Surf. Physicochem. Eng. Asp. 104 (1995) 217–222. https://doi.org/10.1016/0927-7757(95)03288-2.

[37]   M.J. Rosen, Surfactants and interfacial phenomena, Wiley-Interscience, Hoboken, N.J., 2004.

[38]   F. Bouton, M. Durand, V. Nardello-Rataj, A.P. Borosy, C. Quellet, J.-M. Aubry, A QSPR Model for the Prediction of the "Fish-Tail" Temperature of CiE4/Water/Polar Hydrocarbon Oil Systems, Langmuir. 26 (2010) 7962–7970. https://doi.org/10.1021/la904836m.

[39]   A. Graciaa, J. Lachaise, J.G. Sayous, P. Grenier, S. Yiv, R.S. Schechter, W.H. Wade, The partitioning of complex surfactant mixtures between oil/water/microemulsion phases at high surfactant concentrations, J. Colloid Interface Sci. 93 (1983) 474–486.

[40]   A. Graciaa, J. Andérez, C. Bracho, J. Lachaise, J.-L. Salager, L. Tolosa, F. Ysambertt, The selective partitioning of the oligomers of polyethoxylated surfactant mixtures between interface and oil and water bulk phases, Adv. Colloid Interface Sci. 123–126 (2006) 63–73. https://doi.org/10.1016/j.cis.2006.05.015.

[41]   R.E. Anton, J.M. Andérez, C. Bracho, F. Vejar, J.L. Salager, Practical Surfactant Mixing Rules Based on the Attainment of Microemulsion–Oil–Water Three-Phase Behavior Systems, in: R. Narayanan (Ed.), Interfacial Process. Mol. Aggreg. Surfactants, Springer Berlin Heidelberg, Berlin, Heidelberg, 2008.

[42]   S. Burauer, T. Sachert, T. Sottmann, R. Strey, On microemulsion phase behavior and the monomeric solubility of surfactant, Phys. Chem. Chem. Phys. 1 (1999) 4299–4306. https://doi.org/10.1039/a903542g.

[43]   G. Catanoiu, E. Carey, S.R. Patil, S. Engelskirchen, C. Stubenrauch, Partition coefficients of nonionic surfactants in water/n-alkane systems, J. Colloid Interface Sci. 355 (2011) 150–156. https://doi.org/10.1016/j.jcis.2010.12.002.

[44]   M. Ben Ghoulam, N. Moatadid, A. Graciaa, J. Lachaise, Quantitative Effect of Nonionic Surfactant Partitioning on the Hydrophile−Lipophile Balance Temperature, Langmuir. 20 (2004) 2584–2589. https://doi.org/10.1021/la030306u.

[45]   E. Illous, J.F. Ontiveros, G. Lemahieu, R. Lebeuf, J.-M. Aubry, Amphiphilicity and salt-tolerance of ethoxylated and propoxylated anionic surfactants, Colloids Surf. Physicochem. Eng. Asp. 601 (2020) 124786. https://doi.org/10.1016/j.colsurfa.2020.124786.

[46]   S. Zarate-Muñoz, F. Texeira de Vasconcelos, K. Myint-Myat, J. Minchom, E. Acosta, A Simplified Methodology to Measure the Characteristic Curvature (Cc) of Alkyl Ethoxylate Nonionic Surfactants, J. Surfactants Deterg. 19 (2016) 249–263.

[47]   A. Witthayapanyanon, J.H. Harwell, D.A. Sabatini, Hydrophilic–lipophilic deviation (HLD) method for characterizing conventional and extended surfactants, J. Colloid Interface Sci. 325 (2008) 259–266. https://doi.org/10.1016/j.jcis.2008.05.061.